Geological Society of America
Special Paper 398
2006

From weather to climate—Seasonal and interannual variability of storms and implications for erosion processes in the Himalaya

Ana P. Barros[†]
Pratt School of Engineering, Civil and Environmental Engineering Department, Duke University, Durham, North Carolina 27708, USA
Sen Chiao
Division of Engineering and Applied Sciences, Harvard University, Cambridge, Massachusetts 02138, USA
Timothy J. Lang
Department of Atmospheric Sciences, Colorado State University, Fort Collins, Colorado 80523, USA
Douglas Burbank
Department of Geological Sciences, University of California, Santa Barbara, California 93106, USA
J. Putkonen
Department of Earth and Planetary Sciences, University of Washington, Seattle, Washington 98195, USA

ABSTRACT

The extent to which orography may be a product of climate-erosion interactions is largely unknown. One grand challenge is to quantify the precipitation regimes of mountainous regions at the spatial and temporal scales relevant for investigating the interplay of erosion and tectonics in active orogens. In this paper, our objective is to synthesize recent research integrating numerical model simulations, satellite data, and surface observations in the Himalaya to elucidate the role of weather and climate in mountain evolution. We focus on the seasonal and interannual space-time variability of precipitation in the Great Himalayas by studying two preeminent storm regimes in detail—monsoon onsets and depressions in general, and wintertime Western Disturbances (cold season events). High-resolution simulations of heavy precipitation storms for two monsoon onset conditions (1999 and 2001) and one wintertime storm (2000) are used to illustrate the complex patterns of interaction between the mountains and the atmosphere, and to show how these affect the spatial distribution of precipitation. Along with observations from an existing ground-based network, these simulations provide unique insights into the space-time features of seasonal and interannual variability of precipitation. Our analysis indicates that the trajectory of monsoon storms during onset events exerts a strong control on the precipitation amounts and rainfall penetration into the rain shadow. Spatial variability of subsequent storm tracks in any given year helps explain the interannual variability of monsoon precipitation. Both observational data and our simulations define striking spatial variability in precipitation on upwind and downwind flanks of ridges that project into obliquely impinging storms. Specifically, as southeasterly monsoon winds encounter north-south oriented ridges, forced lifting of moist air enhances precipitation on the upwind flanks, whereas less precipitation occurs on downwind flanks. This variability

[†]Email: barros@duke.edu.

Barros, A.P., Chiao, S., Lang, T.J., Burbank, D., and Putkonen, J., 2006, From weather to climate—Seasonal and interannual variability of storms and implications for erosion processes in the Himalaya, *in* Willett, S.D., Hovius, N., Brandon, M.T., and Fisher, D., eds., Tectonics, Climate, and Landscape Evolution: Geological Society of America Special Paper 398, p. 17–38, doi: 10.1130/2006.2398(02).

is observed at spatial scales as short as ~10 km—a distance equivalent to the spacing of major ridge crests. Because infrequent, singular storm events appear to control the mass input to glaciers, and may determine the frequency and spatial distribution of landslides, these findings provide physically based insight into decoupling high-frequency (seasonal to interannual time scales) from low-frequency (multidecadal to centennial and longer time scales) signals in the interpretation of climate and erosion records in the Himalayas. Furthermore, this research suggests that integrative studies aimed at unraveling the role of climate in landscape evolution must include consideration of storm frequency and intensity along with spatial variability at scales consistent with regional climate forcing.

Keywords: precipitation, orography, landform, climate, erosion.

INTRODUCTION

Mountain belts evolve as the product of tectonics interacting with erosion and weathering processes, which are determined by regional hydrology and hydrometeorology, especially the precipitation regime in the case of humid climates. At steady state, removal of landmass by erosion is compensated by isostatic compensation and tectonically driven rock uplift. In turn, mountains strongly affect climate at regional and even global scale by functioning as obstacles to atmospheric circulation, as elevated heat sources via the production of latent heating of orographic precipitation upwind, and by changing the nature of water and energy exchanges between continental surfaces and the atmosphere via either increased snow cover, elevated plateaus, or the establishment of rain shadow deserts. As the topography rises, precipitation changes (increases upwind, decreases downwind), and, at spatial scales ≥100 km, so does erosion (forming deep valleys with elevated peaks upwind [the Himalayan range], allowing elevated plateaus to form downwind [the Tibetan Plateau]). At the scale of millions of years, spatial and temporal changes in the climate regime, changes in spatial and temporal characteristics of erosion processes, and isostatic rebound and rock uplift interact to determine the evolution and form of mountains (Pinter and Brandon, 1997; Molnar et al., 1993).

One question of interest is whether the critical erosion events occur as pulses of catastrophic magnitude (flash floods and debris flows, landslides) associated with infrequent heavy precipitation events, or whether they can be interpreted in terms of "uniform" along-range average erosion rates over long periods of time (Montgomery and Brandon, 2002). In this paper, we discuss evidence suggesting that the former can be a fundamental erosion mode in the Himalayas, which would explain why small-scale erosion studies that fail to capture the relevant spatial variability of climate forcing might not elucidate the role of erosion in mountain evolution (Burbank et al., 2003). This erosional response, we argue, is related to the regional climate and how the mountain range interacts with the atmospheric circulation. Elsewhere (e.g., the Washington Cascades), average long-term coupling of erosion and climate may be dominant (Reiners et al., 2003). Nevertheless, Hodges et al. (2004) pointed out the close spatial correlation between evidence for active faulting and the maxima of annual precipitation in the Annapurna Range in the central Himalayas. Such a spatial association indicates possible coupling between erosion and deformation around the center of mass of orographic precipitation at geological time scales.

Ice-core records (oxygen isotope ratios and chemical composition) have been increasingly used to characterize the low-frequency variability of precipitation in the Himalayas, and by extension, the South Asian Monsoon (Thompson et al., 2000; Zhao and Moore, 2002; Duan and Yao, 2003). The working hypothesis is that precipitation varies linearly with elevation (either positively or negatively) and that all or the overwhelming majority of the precipitation at glacier locations takes place during the monsoon. We propose in this study that, whereas such data may describe the low-frequency variability of the monsoon at multidecadal to centennial temporal scales, the information content of the records must be deconvolved into high- (seasonal to interannual) and low-frequency modes of variability before attempting a process-based interpretation of the underlying phenomena. Specifically, we show that in the hydrometeorological rain shadow of the central Himalayas (the region of elevated peaks and valleys where most glaciers are located, which lies northward of the precipitation maximum), the contribution of monsoon precipitation to annual accumulation decreases very rapidly with altitude, while the contribution of relatively infrequent wintertime snowstorms increases and dominates spatial and interannual variability. Furthermore, we show that the monsoon contribution to precipitation totals in the hydrometeorological rain shadow is controlled by the strength and path of monsoon depressions originating in the Bay of Bengal, and by monsoon onsets in particular, thus exhibiting high interannual variability, not only in magnitude, but also in spatial distribution. In this context, key issues for the interpretation of centennial-scale climate variations from glacier records become (1) the number and timing of storms that contribute to the observed accumulation, and (2) the definition of non-stationarity and dominant time scales of climate behavior.

These characteristics are important not only from the perspective of elucidating current climate variability, but also for testing the interpretations of climate-tectonics interactions that often rely on average annual precipitation to describe climate controls on landform evolution. A key implication of this study is that, in the range of seasonal to interannual time scales, the atmo-

spheric moisture flux that nurses existing glaciers arrives via chaotic pulse-like events (monsoon depressions, wintertime storms) with high space-time variability, and therefore is fundamentally non-stationary. Such behavior redirects attention to seasonal and interannual variability of storm frequency and intensity and to how these affect the temporal and spatial variability of precipitation as related to climate controls of erosion in the Himalayas.

In this manuscript, we document the spatial features of three storms, including two distinct monsoon onsets (1999 and 2001) and one typical wintertime storm. For this purpose, we rely on numerical simulations using a regional model at very high spatial resolution (1.86 km, unprecedented in this region of the world), which is necessary to resolve the significant cloud features (Barros et al., 2004). The modeling results are presented in the context of extensive data analysis and synthesis from previous diagnostics studies (Barros et al., 2000, 2004; Lang and Barros, 2002, 2004; Barros and Lang, 2003a; Magagi and Barros, 2004). First, we review findings from previous work in order to characterize monsoon weather, and to establish the observational evidence of seasonal and interannual climate variability in the Himalayas. Second, spatial fields of relevant atmospheric variables (wind fields and cloud liquid water) obtained from the numerical simulations are used to illustrate the role of orography in organizing clouds and rainfall on the Himalayan range under different large-scale environmental conditions. We conclude by discussing the implications of our findings for the characterization of erosion processes in the Himalayas.

MONSOON WEATHER IN THE HIMALAYAS

Every summer in South Asia, the thermal contrast between the slowly warming ocean and the rapidly warming land accelerates vertical air flow over the land and thereby drives the landward flow of moisture that underpins the monsoon. The large, high-altitude mass of the Tibetan Plateau greatly strengthens this land-sea contrast regionally, and serves to enhance the intensity of the monsoon. In the Indian subcontinent, the onset of the Southwest (SW) monsoon takes place after a region of strong low-level moisture flux associated with southwesterly cross-equatorial flows off the coast of Somalia (i.e., the Somali jet) becomes well developed (e.g., Krishnamurti et al., 1981; Tang and Reiter, 1984, among others). An elongated area of low pressure, the monsoon trough, becomes established roughly parallel to the Himalayan range, and subsequent monsoon activity is associated with the development of low-pressure systems (mesoscale vortices) along the monsoon trough. Monsoon activity along the south-facing slopes of the Himalayas is associated with the development and westward propagation of monsoon depressions originating from the Bay of Bengal (Das, 1987; Lang and Barros, 2002). Ultimately, the path of Bay of Bengal depressions is determined by the position of the monsoon trough, the Coriolis effect (northward deflection), the origin and strength (vorticity) of the monsoon systems, and their interactions with the land surface as they travel over northern India.

A comprehensive compilation and analysis of observations from a dense hydrometeorological network operating since 1999 in the Marsyandi River basin in central Nepal (Barros et al., 2000; Fig. 1A) revealed the complexity of the relationship between elevation and precipitation in the central Himalayas (Barros et al., 2004), including (1) weak altitudinal gradients of annual rainfall between 1000 and 4500 m; (2) strong ridge-to-ridge zonal (east-west) gradients of monsoon rainfall (1500 mm/5 km); (3) strong ridge-valley gradients during rain storms, especially in the case of deep valleys (elevation differences > 1000 m) and steep hillslopes (70%); and (4) strong altitudinal gradients in rainfall intensity and duration (convective versus stratiform), with longer (shorter) durations and lower (higher) intensities at higher (lower) elevations along the ridges. High elevations (>3000 m above sea level [asl]) can receive up to 40% of their annual precipitation as snowfall during the winter, with the highest-altitude stations (~4000 m asl and above) accumulating the most total winter precipitation (Lang and Barros, 2004; Barros et al., 2004). A comprehensive summary of the observations is presented in Figure 1B. Note that there is a rapid decrease of precipitation amount in the region of the hydrometeorological shadow, and that the spatial gradient associated with this decrease is much stronger for rainfall than for snowfall. Observed cumulative rainfall reaches minimum values well upwind of the topographic divide, thus raising questions with regard to the relative contribution of monsoon vis-à-vis wintertime precipitation to modern glaciers.

At the scale of the Himalayan range, the spatial and temporal variability of precipitation was investigated using NASA-TRMM (National Aeronautics and Space Administration Tropical Rainfall Measurement Mission) and Meteosat-5 (a geostationary satellite maintained by the European Meteorological Satellites Organization, EUMETSAT) analysis data products (Barros et al., 2000, 2004). Scaling analysis of collocated orography and cloudiness fields uncovered two distinct types of orographic controls at different spatial scales: a synoptic-scale control (~300 km) associated with the overall terrain envelope and the major river valleys that cut through the mountains connecting the Indian subcontinent and the Tibetan Plateau; and a mesoscale control characterized by high interannual and spatial variability linked to the topology of the succession of multiscale ridges and valleys along the southern slopes of the Himalaya (5–100 km). Depending on the actual complexity of the terrain, the variance of cloudiness and its scaling behavior reflected the ridge density, as well as its altitudinal range (Barros et al., 2004).

The synoptic and mesoscale dynamics of monsoon and wintertime storms were analyzed based on field campaign data, historical radiosonde records, ECMWF (European Center for Medium-Range Weather Forecasts), and NCEP (National Centers for Environmental Prediction) reanalysis products and high-resolution numerical models (Lang and Barros, 2002, 2004; Barros, 2004; Lang, 2003a). Through these studies, three preeminent weather regimes can be identified that can help to explain the seasonal and interannual variability of precipitation: (1) monsoon onset depressions (Lang and Barros; 2002; Barros and

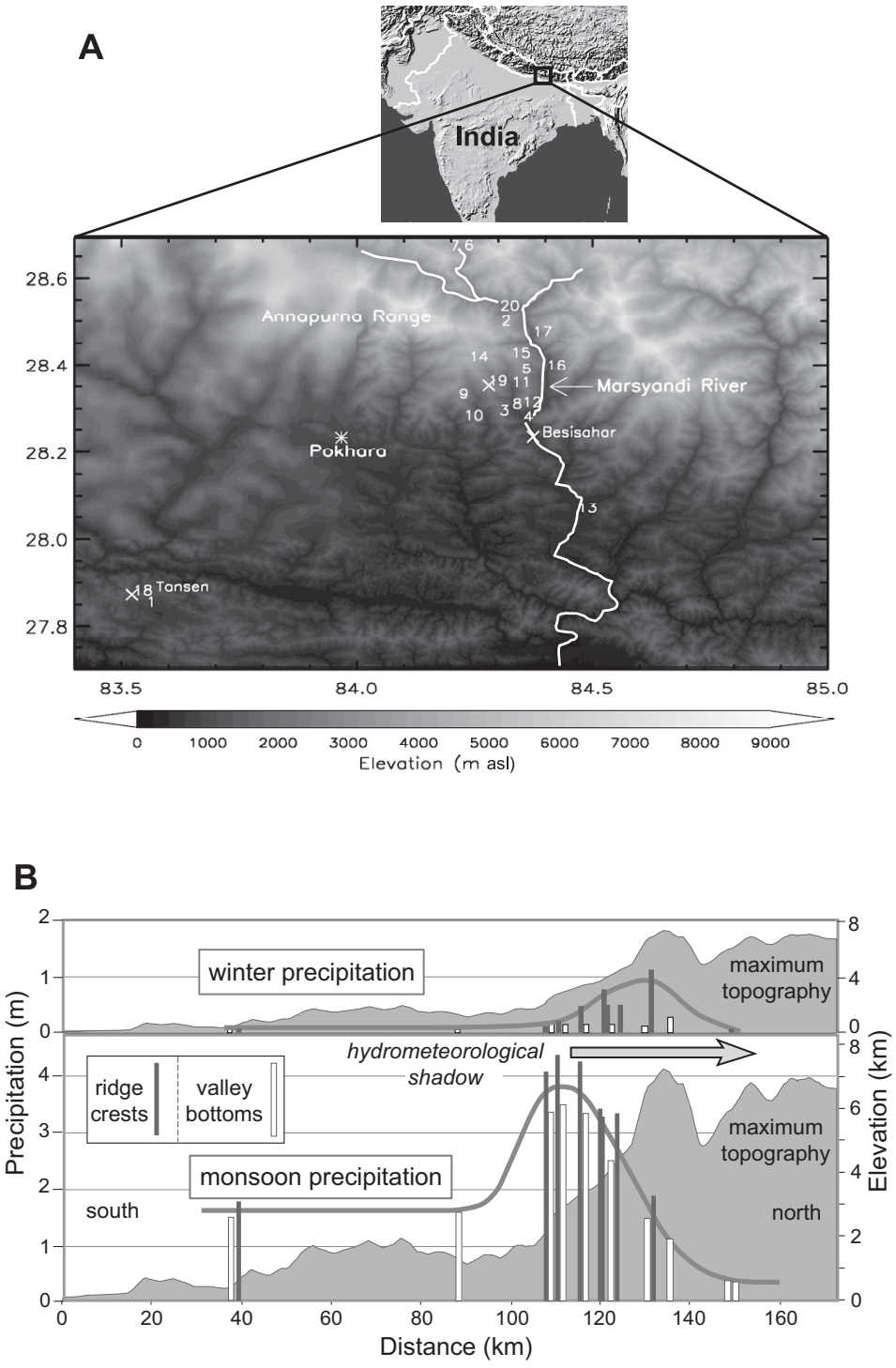

Figure 1. (A) Topography of the Marsyandi River basin. The lower map shows locations of the hydrometeorological stations in the network. The upper map shows the location of the network relative to the Indian subcontinent. (B) Cumulative summer (bottom panel) and winter (top panel) precipitation and maximum topography (averaged along a 60-km-wide swath) are plotted against distance perpendicular to the Himalayan range crest. Precipitation data were collected at 20 stations from 1999 to 2002. The summer monsoon precipitation increases dramatically at all measured elevations as the maximum elevation of the orogen climbs above 2000 m. It then drops off rapidly to the north. Precipitation on the ridge crests is consistently 10%–20% greater than in the valley bottoms. Winter precipitation (top panel) shows a much greater ridge-to-valley contrast, lower precipitation amounts, and a peak of precipitation offset toward the range crest.

Lang, 2003a); (2) mesoscale convection organized by orography (Barros and Lang, 2003a; Barros et al., 2004); and (3) wintertime storms associated with a low-pressure center over the Hindu Kush mountains, the so-called Western Disturbances (Lang and Barros, 2004). We focus on 1 and 3, respectively. Monsoon onset depressions are hereafter referred to as "onset events," and wintertime storms are hereafter referred to as "snow storms" or "cold-season events." The development of convective activity aligned with topographic features is characterized by a strong diurnal cycle, and is particularly strong during the active phases of the monsoon, including onset events (Barros and Lang, 2003a; Barros et al., 2004).

Monsoon onsets consist of heavy, multiday rain events, which are precursors to the subsequent arrival of daily to near-daily rainfall for the rest of the summer season. The onset takes place when strong mesoscale depressions originating from the Bay of Bengal in the first half of June interact with easterly vertical shear forced by the mountains, establishing an asymmetric secondary circulation with strong near-surface upslope (southerly) flow and return flow (northerly) at 600–700 hPa (Lang and Barros, 2002; Barros and Lang, 2003a). Interactions with local topography serve to organize convective activity along the foothills of the Himalayas. At the northerly stations (e.g., 5, 14, and 15 in Fig. 1A), total rainfall during onset events can amount up to 30% of the overall monsoon total (Lang and Barros, 2002, 2004). A climatological analysis of the track of these storms (Fig. 2) shows that they vary widely from year to year (Das, 1987; Lang and Barros, 2002). The southward shift in the year 2000 monsoon track (Fig. 2) caused the 2000 onset rainfall to be up to the 50% less than in 1999. The onset precipitation was even less in 2001, as the onset depression remained south of the range.

As described by Barros and Lang (2003a), monsoon depressions tend to form along the monsoon trough over the Bay of Bengal, and to propagate westward on the northern flank of the

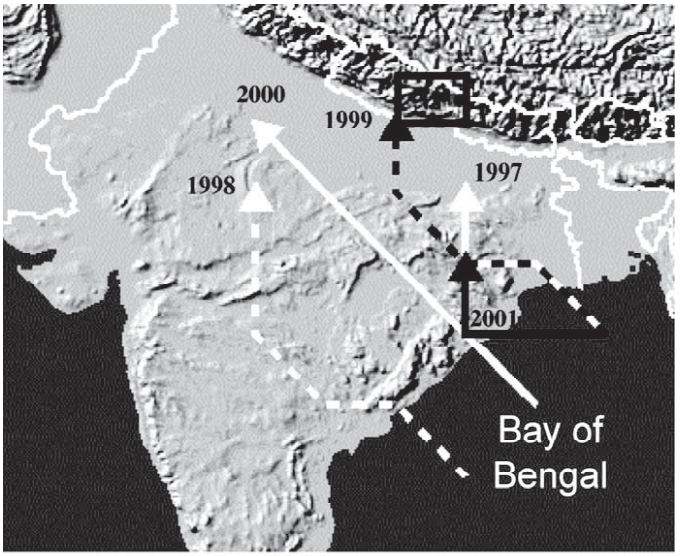

Figure 2. Storm tracks for the Nepal onset depressions (1997–2001). Tracks were determined by the locations of the 850 hPa (~1.5 km) relative vorticity maxima in the European Center for Medium-Range Weather Forecasts (ECMWF) data. The black box surrounds the location of the Marsyandi network. (Image is reproduced from Lang and Barros, 2002.)

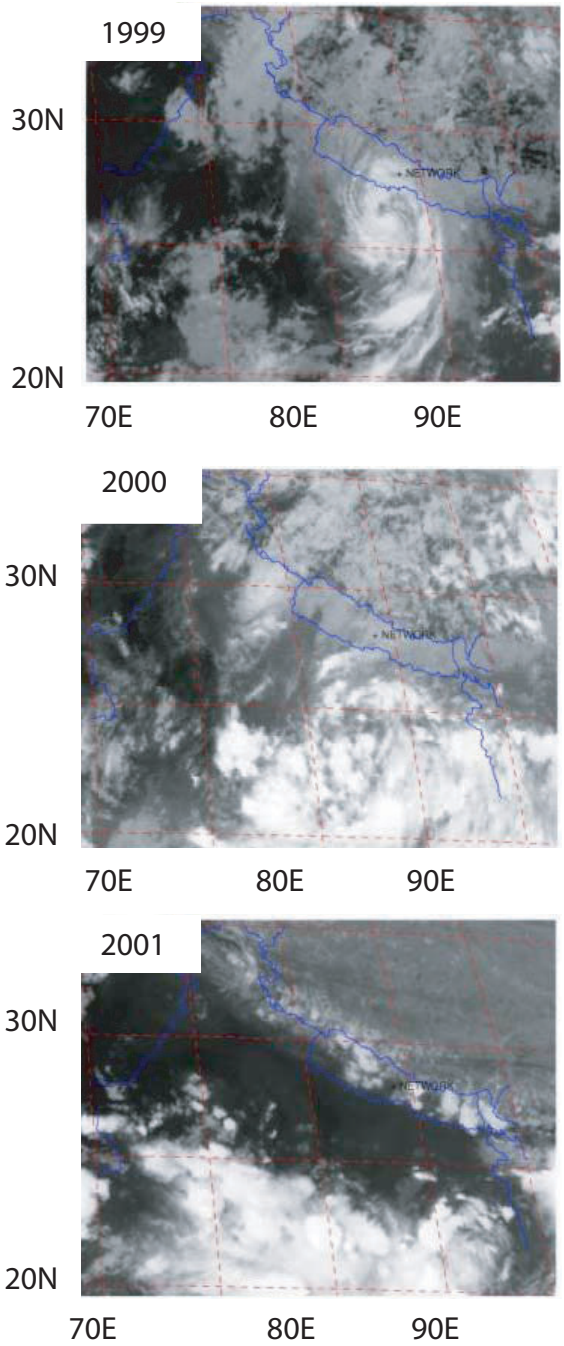

Figure 3. Infrared imagery from Meteosat-5 showing representative cloud fields for three monsoon onsets: 1999, 2000, and 2001. The location of the Marsyandi network is also marked.

westerly jet over the Indian subcontinent. When the depressions follow a trajectory farther away from the Himalayas (as in 2000, Fig. 2), the interactions with the easterly vertical shear along the Himalayas are weakened, thereby decreasing convergence and keeping the depressions away from the Himalayan range and favoring disorganized convection over northern India.

Satellite imagery (Fig. 3) readily depicts cloudiness fields during three monsoon onsets (1999, 2000, and 2001). The climatology of depression strength and motion track influences not only rainfall amounts, but also the spatial variability of precipitation, especially the extent to which rain bands associated with these depressions penetrate northward beyond the leading mountain peaks. Because similar, though generally weaker, depressions occur during the active phases of the monsoon from June to September, this analysis has implications not only for monsoon onsets, but also for the spatial distribution of rainfall over the course of the entire monsoon season.

Lang and Barros (2004) focused their attention on cold-season events. They found that significant snowstorms are associated with terrain-locked low-pressure systems that form when an upper-level disturbance passes over the topographic notch (Fig. 4A) formed by the Himalayas and Hindu Kush mountains (Western Disturbances), causing upper-level SW flow over central Nepal and topographically forced precipitation over extended areas at high elevations. They developed a 30 yr (1973–2002) climatology of these "notch" depressions, which revealed significant interannual variability in central Himalayan winter storms, in particular with regard to the number of such storms per year (fewer than six on average), from years when none occurs (1987, coincidentally a weak monsoon year) to over ten per year.

MODELING STUDIES

Observational data currently available, either ground-based or from satellites, do not provide a multiscale perspective of space-time variability of precipitation on the Himalayan range. Hydrometeorological networks such as the Marsyandi (Fig. 1A) can provide detailed information over the small area covered by the network only. As an indirect measure of precipitation, satellite data present substantial retrieval challenges in regions of complex terrain where precipitation effects are difficult to separate from terrain and snow-cover effects, a difficulty that is compounded with inadequate sampling frequency in either space or time (or both) (Barros et al., 2000; Magagi and Barros, 2004). Model simulations such as those described here allow us to monitor in detail the three-dimensional spatial and temporal evolution of relevant weather systems and their precipitation fields.

Based on analysis and interpretation of observational records (satellite, radiosonde, and rain gauge data), we concluded that onset events provide clear insights on the long-term hydroclimatology of summer monsoon precipitation in the Himalayas. Therefore, we focus on modeling two onset events that are representa-

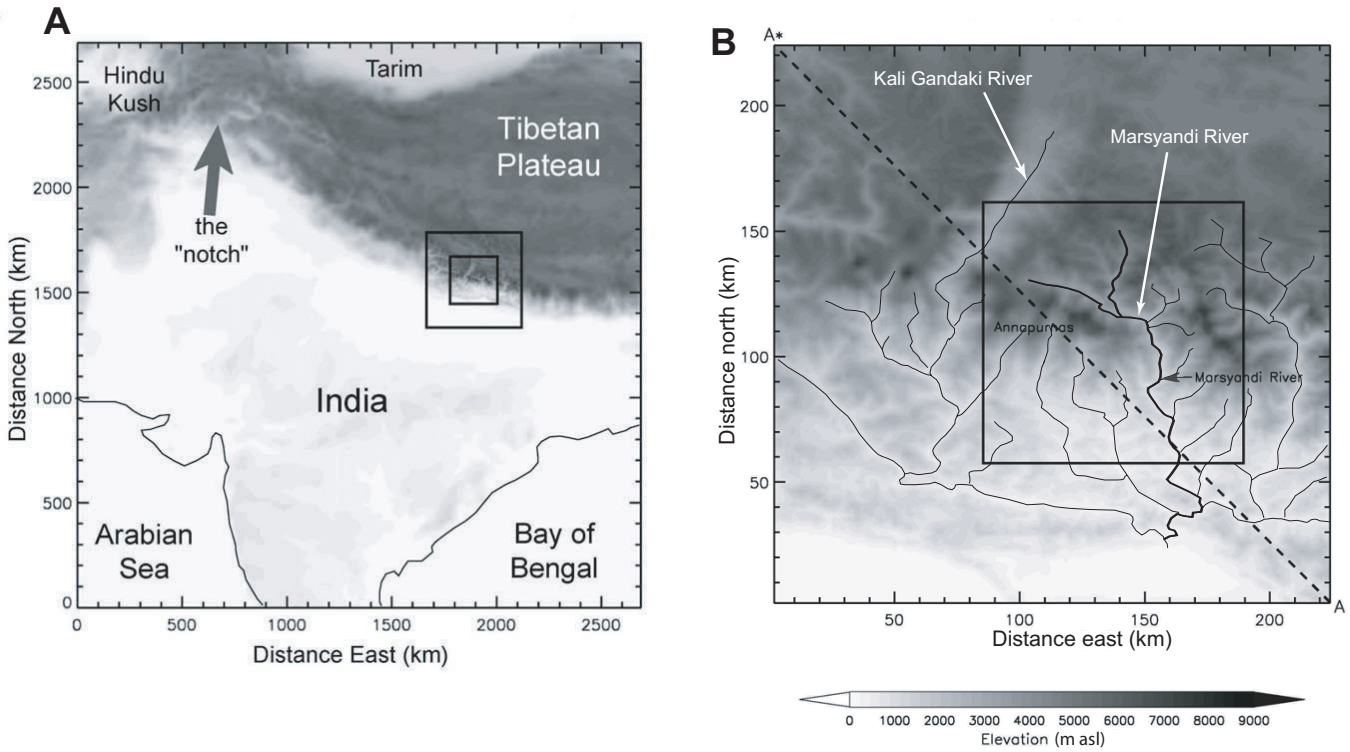

Figure 4. (A) Model computational domain. The grid increments for the three nested meshes are 22.22 km, 3.70 km, and 1.86 km, respectively. (B) Terrain used for the inner domain grid (1.86 km resolution). The rectangular box contains the general area of the hydrometeorological network and current glaciers in central Nepal. The solid line A–A* represents the orientation of the *x-z* cross sections in subsequent analyses.

tive of end members of monsoonal precipitation patterns (1999 and 2001). Furthermore, our research suggests that the character of the ensuing monsoon season correlates with certain characteristics of the monsoon onset event (Barros et al., 2004): a monsoon onset characterized by a well-defined vortex and well-organized convection (e.g., 1999 and 2000) foretells normal or above normal precipitation, with significant penetration of moisture (up to 30% of monsoon total rainfall) into the hydrometeorological shadow in the high Himalayas; whereas a monsoon onset with a weak vortex and widespread disorganized convective activity appears to set the stage for significantly below normal rainfall, especially at high elevations (e.g., 2001). Similarly, we present results for a representative wintertime weather event, specifically a snowstorm in February 2000 (Lang and Barros, 2004). For each case, a description of the synoptic environment of each storm is provided first, followed by a detailed discussion of model results. The analysis of model results will focus on central Nepal (i.e., the network area) where the hydrometeorological network and the glaciers of interest are located.

Description of the Model and Experiment Design

We use a three-dimensional, anelastic, and non-hydrostatic high-resolution model originally introduced by Clark (1979) and Clark and Hall (1991, 1996) in our modeling experiments. Since its original implementation, the model has undergone substantial improvements, and has been particularly successful in studies of small-scale and mesoscale weather phenomena in regions of

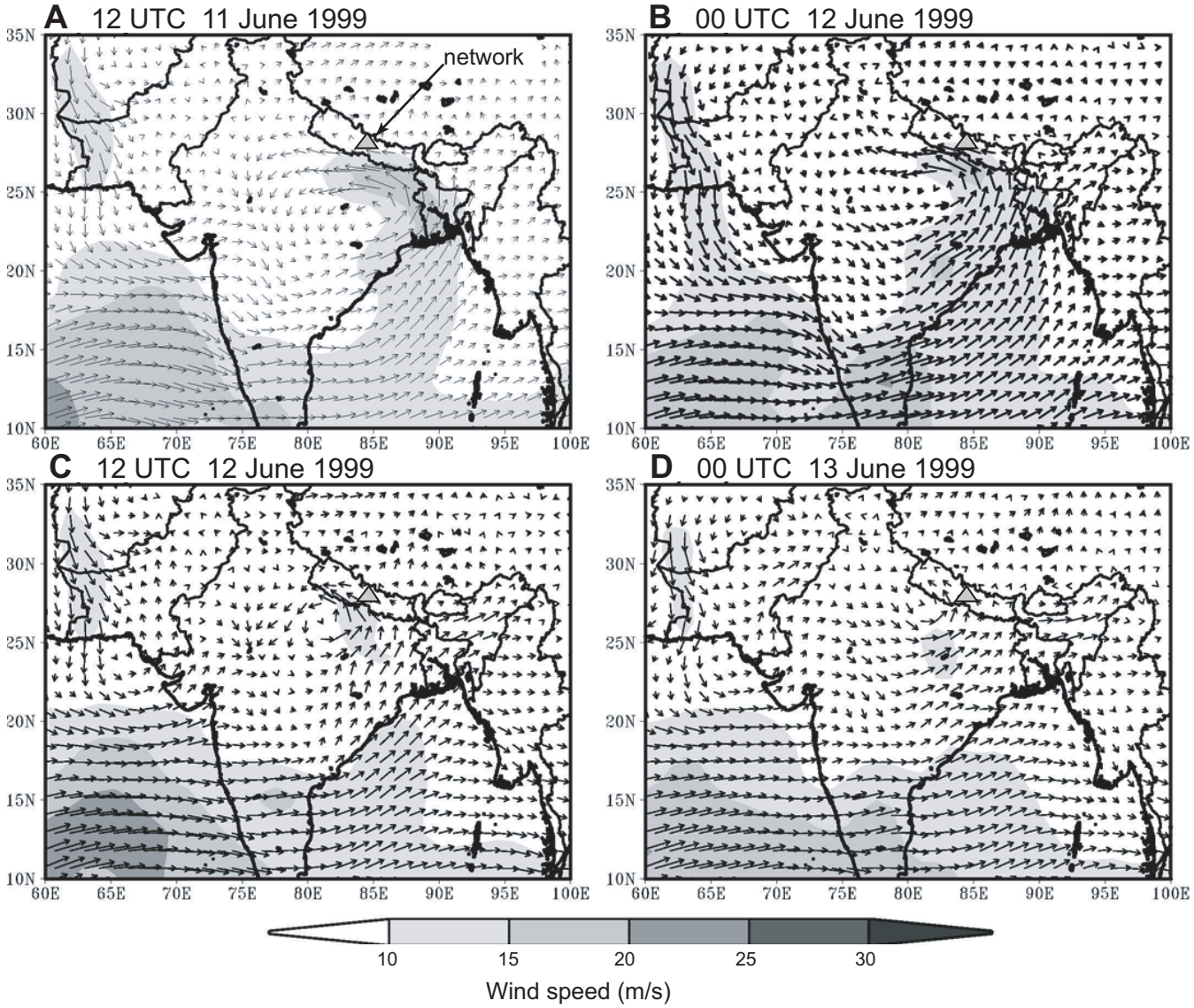

Figure 5. 1999 onset 850 hPa wind streamlines (vectors) and wind speed (shaded) for (A) 12 UTC 11 June, (B) 00 UTC 12 June, (C) 12 UTC 12 June, and (D) 00 UTC 13 June 1999. Gray triangles mark the approximate location of the network. Note that velocities are zero where the terrain height is above 850 hPa (~1.5 km asl).

complex topography, including the Rocky Mountains, the Sierra Madre, and the Himalayas (Clark, 1979; Clark and Hall, 1996; Reinking et al., 2000; Barros and Lang, 2003b; Lang and Barros, 2004, among others).

The model was implemented here using three nested grids. The outer, large-scale domain (22.22 km horizontal resolution) encompassed an area of 2700 × 2700 km, including large portions of the Tibetan Plateau and the Indian subcontinent. The innermost domain (1.86 km horizontal resolution) covered an area of 200 × 200 km, centered on the region where the hydrometeorological network and glaciers are located. The topography used by the model was derived from the Defense Mapping Agency (DMA), United States elevation data, which is available from the Scientific Computing Division of the National Center for Atmospheric Research. Figure 4A displays the topography of the outermost domain with the outline of each of the two inner domains. The model topography for domain 3 (i.e., the inner grid) is representative of the complex local topographic features, with several mountain peaks of the Himalayas higher than 6000 m (Fig. 4B). Time-dependent boundary conditions for model simulations were derived from the European Center for Medium-Range Weather Forecasts (ECMWF) analysis data sets.

In the simulations presented here, the outermost vertical grid increment, Δz, varied smoothly from 50 m at the surface to 200 m at z = 425 m above ground level and increased more gradually to 407 m at 4.15 km above ground level using the stretched vertical coordinate transformation. A modified Kessler (1969) warm rain bulk microphysics parameterization, which predicts the mixing ratios of cloud water (q_c) and rain water (q_r), was used to characterize microphysics. Although this parameterization is lacking in detail necessary to simulate accurate quantitative estimates of precipitation (e.g., ice microphysics are not included), it is adequate to investigate the spatial and temporal evolution of precipitating clouds. Long-wave radiative cooling was described via a combination of the parameterizations of Stephens (1984) and Sasamori (1972). For more information on the implementation of these parameterizations in the model, the reader is referred to Clark et al. (1996). Finally, the version of the model used here does not include land-atmosphere interactions and thus cannot simulate the combined effect of orographically induced ascent

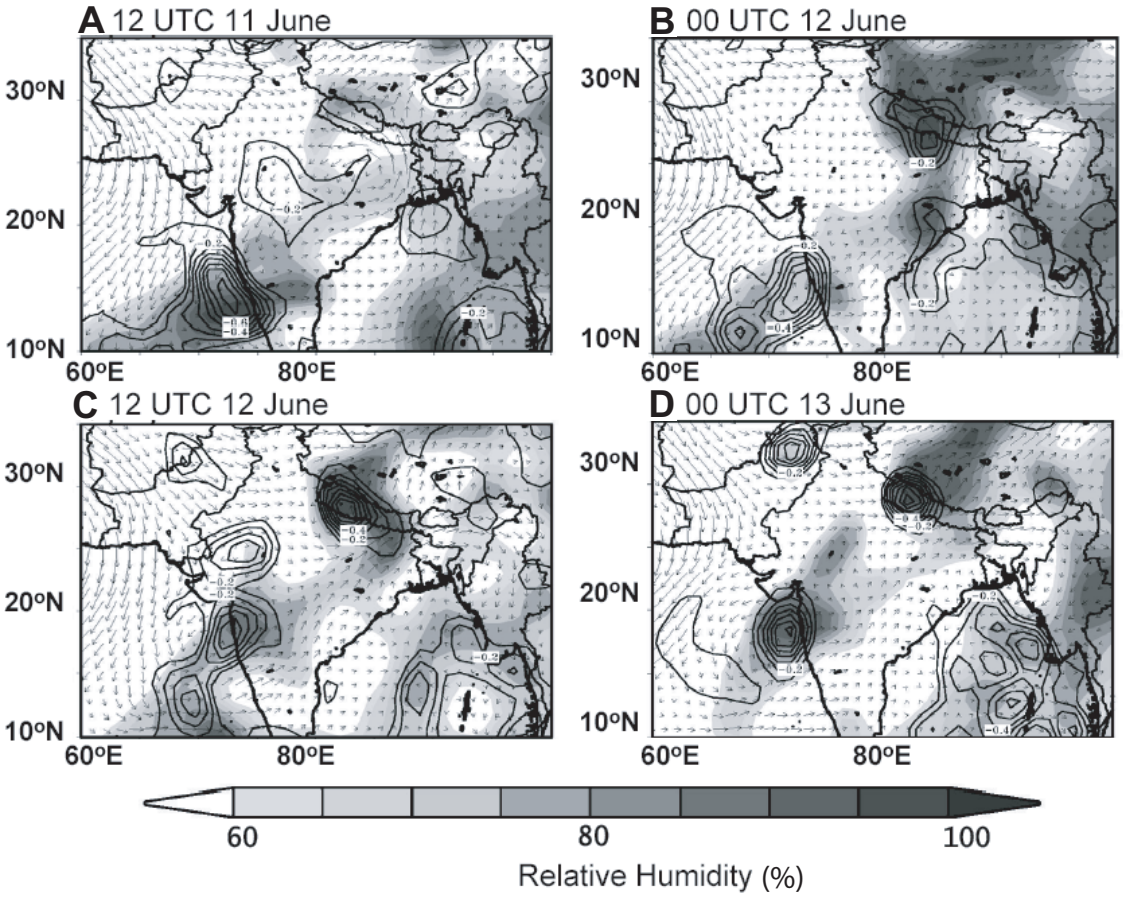

Figure 6. 1999 onset 500 hPa (~5–6 km asl) and relative humidity (RH [%], shaded), horizontal wind streamlines (vectors), and contours of upward vertical wind velocity (0.2 Pa/s ~2 cm/s contour interval; negative velocities are upward; velocity increases from zero at the outermost contour to a maximum at the innermost contour).

and gravity wave dynamics on the stability of the boundary layer, or moisture recycling between the land surface and the lower atmosphere as inferred from analysis of MOHPREX (Monsoon Himalaya Precipitation Experiment) data (Barros and Lang, 2003a).

Overview of Synoptic Conditions

1999 Monsoon Onset

The 1999 monsoon onset in central Nepal was characterized by a low-pressure system (i.e., monsoon depression) that developed in the Bay of Bengal. By 00 UTC on 11 June 1999, this monsoon depression was located near 22.0N, 88.0E, and the low center was ~996 hPa (not shown). Based on 850 hPa winds (~1.5 km in the lower troposphere) from ECMWF objective analysis of model and observations, the evolution of the monsoon depression is depicted in Figure 5 as it moved northwestward toward the central Himalayas at 12 UTC on 11 June (Fig. 5A), 00 UTC on 12 June (Fig. 5B), 12 UTC on 12 June (Fig. 5C), and 00 UTC on 13 June 1999 (Fig. 5D). Note the strong component of flow (>10 m s^{-1}) impinging on central Nepal. Inspection of the vertical structure of horizontal winds, relative humidity distribution, and upward motion fields indicates that the moisture-laden monsoon flow over the mountains extended up to the 500 hPa level (5–6 km in the lower troposphere, Fig. 6), thus implying significant moisture transport to the hydrometeorological network area as well as to the glaciers at higher elevations. The ECMWF analysis fields indicate significant penetration of moisture far into the northern edge of the Himalayan range, consistent with ground observations and IR (infrared) satellite imagery (Barros et al., 2004). Moreover, moisture convergence was enhanced orographically as the incoming air mass reached the mountain slopes (Lang and Barros, 2002; Barros and Lang, 2003a) resulting in the development of a shield-like pattern of mesoscale precipitation with embedded convection, as captured by the TRMM-PR (Tropical Rainfall Measuring Mission- Precipitation Radar) on 12 June 1999 (Fig. 7). The TRMM-PR did not detect precipitation in the northern (rain shadow) area of modern glaciers, and it underestimated rainfall amounts in the network area (Barros et al., 2000). Such systematic underestimation of precipitation at high elevations and in regions of complex terrain in general is a well-known deficiency of satellite precipitation products (TRMM Science Team Working Group Summaries, 2003, available at http://trmm.gsfc.nasa.gov).

2001 Monsoon Onset

The monsoon depression developed in the Bay of Bengal in 12 June 2001 and moved westward toward the Indian subcontinent. The low-pressure center was ~996 hPa before landfall (figure not shown). Associated with this monsoon depression was a southeasterly wind, which brought moist air into the Indian

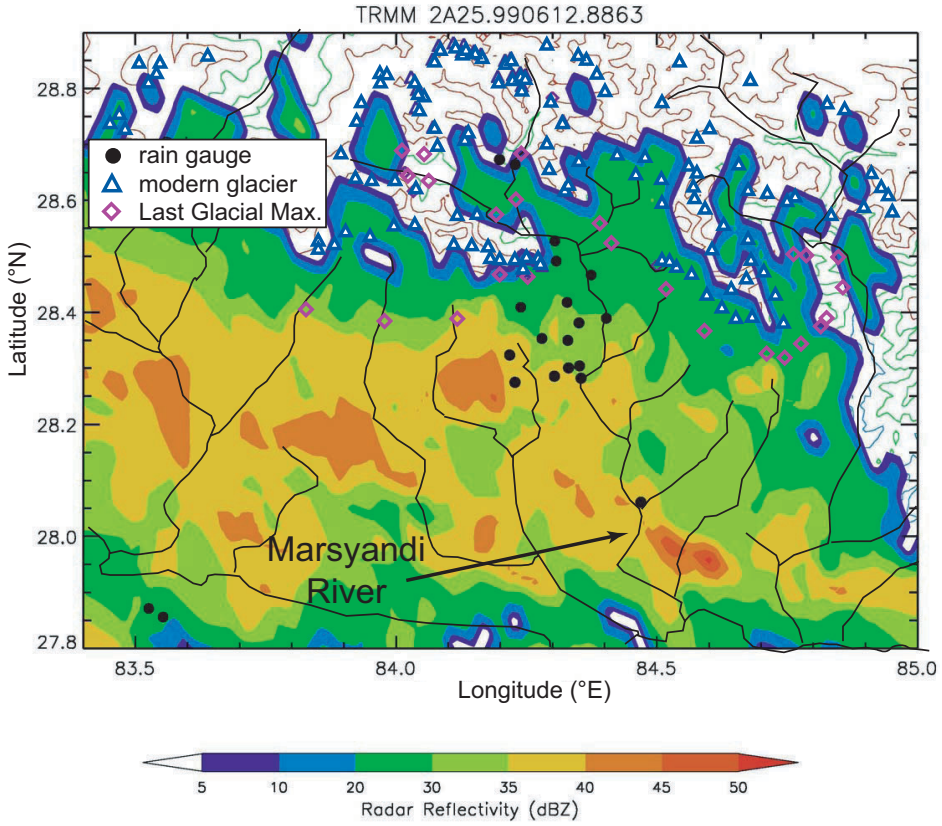

Figure 7. Tropical Rainfall Measurement Mission (TRMM) precipitation radar maximum reflectivity on 12 June 1999. Dark circles indicate positions of hydrometeorological stations shown in Figure 1A. The average location of modern glaciers (triangles) and maximal terminal positions of Late Quaternary glaciers (diamonds) permit assessment of the extent of the remotely sensed precipitation with respect to the glaciers.

subcontinent. On 13 June 2001, the 850 hPa (~1.5 km) height and wind analysis at 00 UTC indicated that the monsoon depression made landfall along the northeast coast of India (Fig. 8A). Twenty-four hours later, by 00 UTC 14 June, the 850 height field clearly showed that the monsoon depression was embedded in the monsoon trough and steered by the flow near the southern periphery of the high-pressure system over the Tibetan Plateau (Fig. 8B). The 500 hPa (~5–6 km) vertical motion and relative humidity fields indicate that strong upward airflow occurred in the western periphery of the monsoon depression (not shown). Subsequently, the monsoon depression moved northwestward away from the central Himalayas.

Although the track of the monsoon depression stayed away from the central Himalayas, significant rainfall (3–6 cm) was observed at the surface network (Barros and Lang, 2003a). The TRMM precipitation radar was able to capture the convection along the periphery of the monsoon depression. TRMM-measured radar reflectivity around 1200 Local Standard Time (LST) 12 June (top panel, Fig. 9) indicates the presence of a strong convective cell near the hydrometeorological network area. By 1200 LST 14 June (Fig. 9, bottom panel), convective activity weakened as the monsoon depression moved further inland, moisture convergence was virtually shut off, and the boundary layer along the Himalayan range became more stable. Once again, negligible precipitation was detected by TRMM at high elevations in the glacier region, as noted previously.

2000 Winter Storm

On 11 February 2000 a snowstorm developed in the Himalayan range, and was detected by ground observations in central Nepal (Lang and Barros, 2004). The 850 hPa height and wind fields from ECMWF analyses on 00 UTC 11 February 2000 (Fig. 10A) show a shallow depression that developed over the western Himalayas when a westerly trough passed over the region between the Himalayas and the Hindu Kush in the northwestern corner of the Indian subcontinent (Fig. 10A). Twelve hours later (Fig. 10B), this system, which drew moisture from the Arabian Sea, intensified as the trough moved eastward. During this period, a strong south-southeasterly low-level jet accompanied the eastward-moving deep trough. Orographic lifting led to the redistribution of the incoming moisture flux and enhancement of precipitation processes over the mountains. At the ground stations in central Nepal, the snow records indicate snow depth accumulations from 5.5 to 22.2 cm (snow density ~0.5; Lang and Barros, 2004). During the life cycle of the system, strong upward motion was observed over the western Himalayas and the Hindu Kush mountains in the ECMWF analysis data set, while strong westerlies over the Indian subcontinent encroached against the Himalayas. The TRMM satellite did not have an overpass concurrently with this event.

Results of Numerical Experiments

1999 Monsoon Onset

A 36 h simulation was run from 00 UTC 12 June to 12 UTC 13 June 1999 for the 1999 monsoon onset event. Time-dependent initial and lateral boundary conditions from ECMWF were imposed at 6 h intervals. Figures 11A and 11B show the simulation results 1.5 km above the ground surface for the outer domain (Δx = 22.22 km) at 12 UTC (18 LST) 12 June, and 00 UTC (06 LST) 13 June 1999, respectively. On 12 UTC 12 June 1999, the

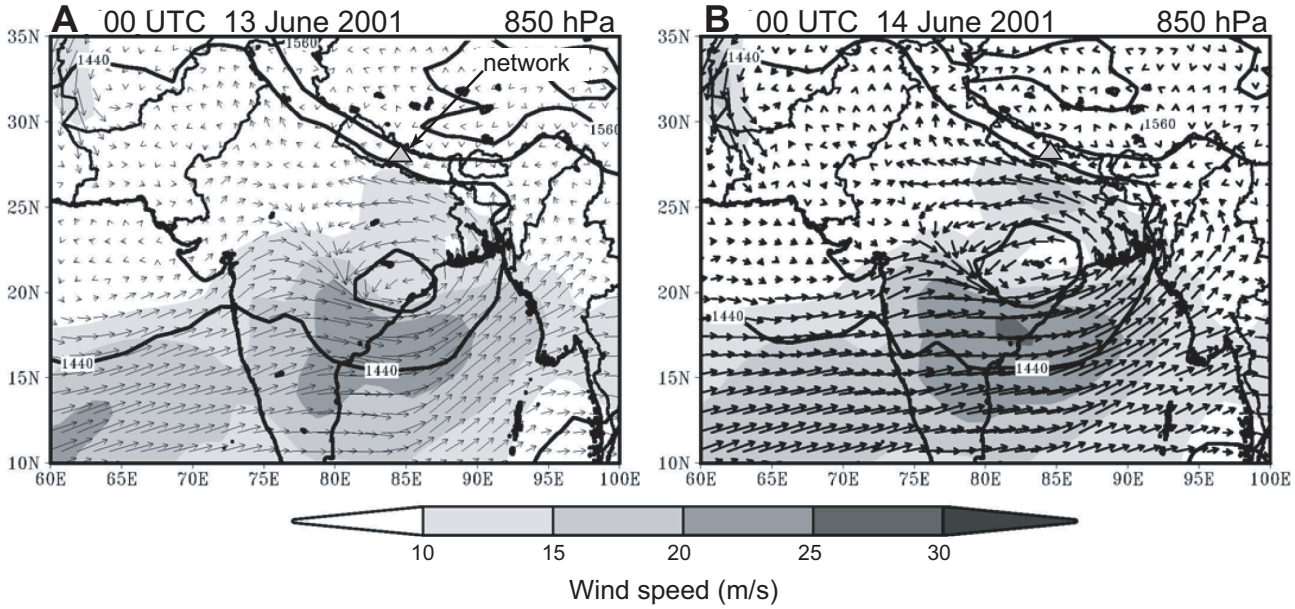

Figure 8. 850 hPa wind fields from European Center for Medium-Range Weather Forecasts (ECMWF) analysis at (A) 00 UTC 13 June, and (B) 00 UTC 14 June 2001, streamlines (vectors), wind speed (shaded), and geopotential heights (labeled contours at 120 m interval). Note that velocities are zero where the terrain height is above 850 hPa (~1.5 km asl).

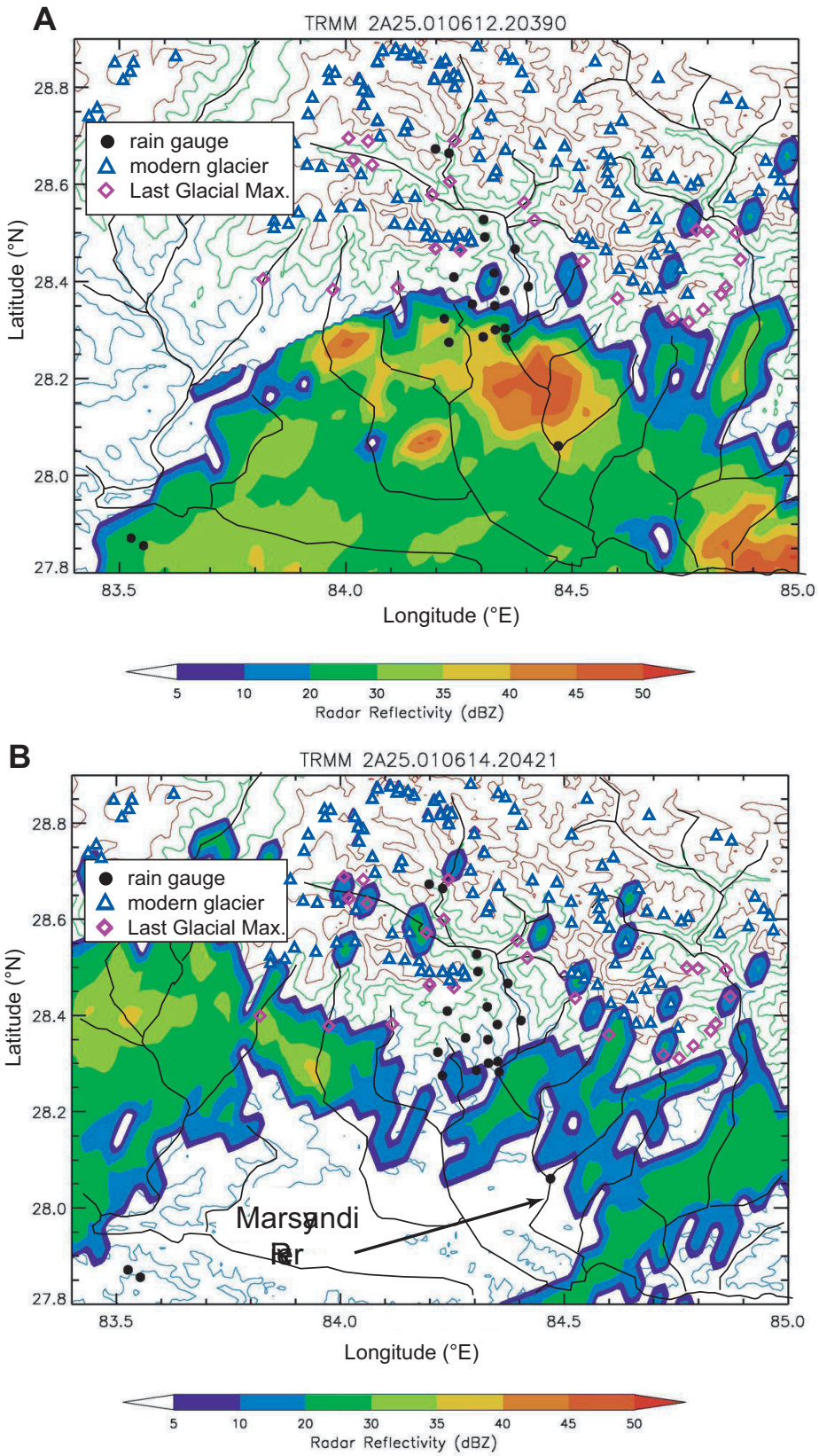

Figure 9. (A) Tropical Rainfall Measurement Mission (TRMM) precipitation radar maximum reflectivity at 06 UTC 12 June 2001. (B) TRMM precipitation radar maximum reflectivity at 06 UTC 14 June 2001. Note that, in comparison to Figure 7, northward moisture penetration is greatly reduced. Symbols are as in Figure 7.

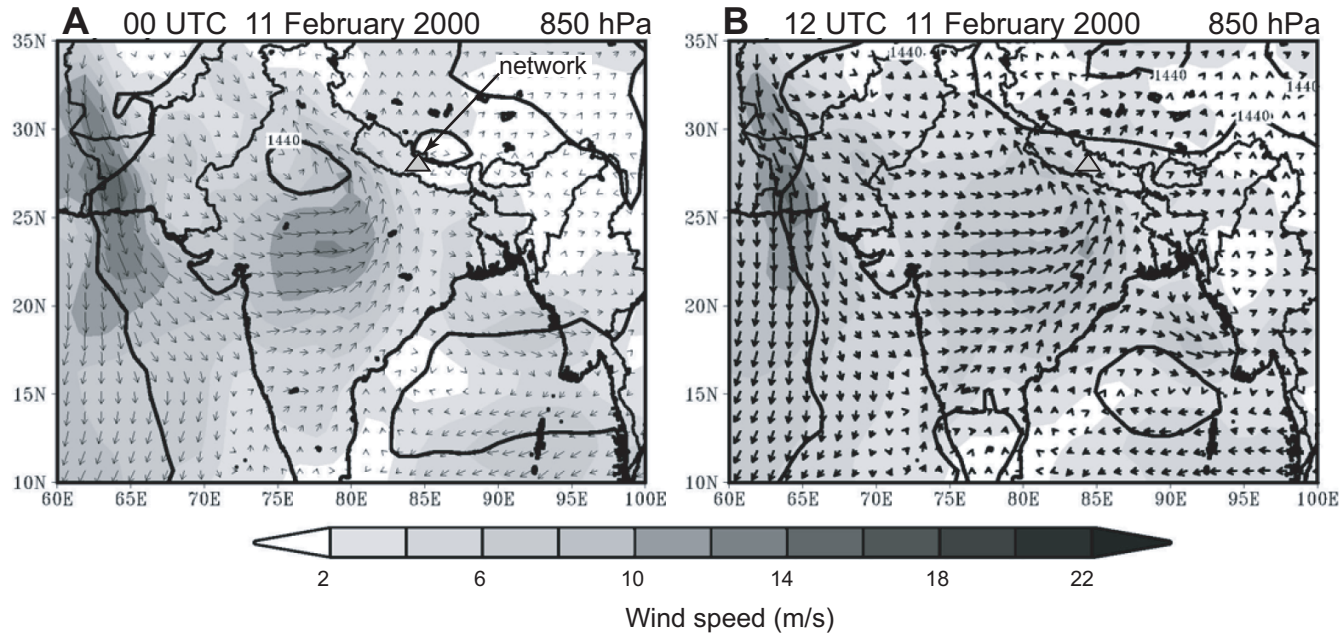

Figure 10. 850 hPa horizontal wind streamlines (vectors) and wind speed (shaded) from European Center for Medium-Range Weather Forecasts (ECMWF) analysis at (A) 00 UTC and (B) 12 UTC 11 February 2000. Gray triangles mark the approximate location of the network. Note that velocities are zero where the terrain height is above 850 hPa (~1.5 km asl).

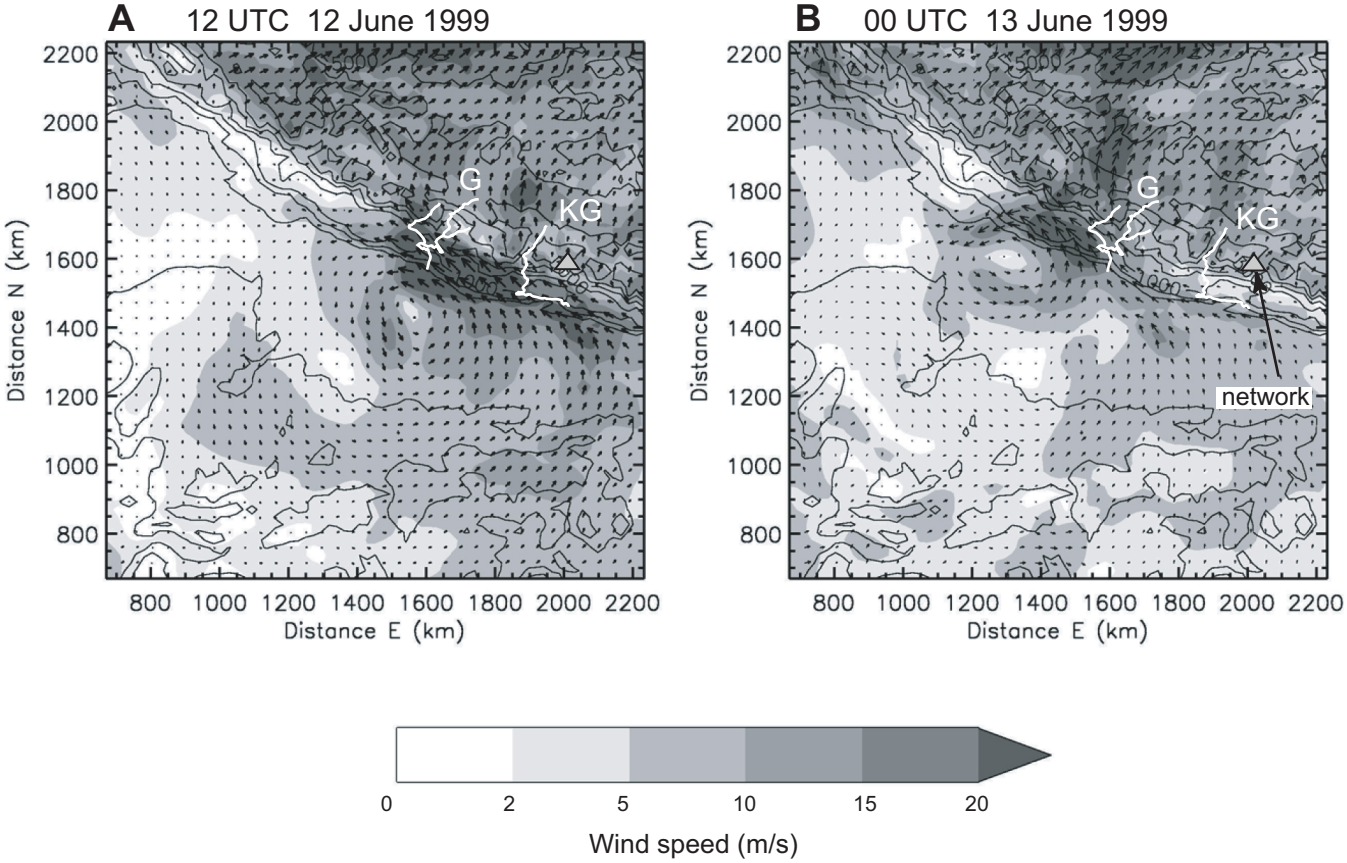

Figure 11. Simulated horizontal wind streamlines (vectors) and wind speed (shaded) 1.5 km above the ground surface for the outer model domain (domain 1, 22.22 km grid resolution) at (A) 12 UTC 12 June 1999, and (B) 00 UTC 13 June 1999. Note the strong northward flow toward the Tibetan Plateau along the Kali Gandaki (KG) and Ghaghra (G) drainages, whereas a region of more stagnant air lies between them. Contours show orography in increments of 1000 m.

model captured correctly the position of the core of the monsoon depression, placed over central Nepal at ~26°N (compare Fig. 3 with Fig. 11A). An impinging wind on the order of 20 m s^{-1} was simulated at that time. The track and the circulation of the monsoon depression are quite well reproduced as it moved northwestward along the Himalayas (Fig. 11B). The moist Froude number Fw is ~0.5 ($Fw = U/N_w h_m$, where U is the basic flow speed near the mountain, N_w is the moist static stability of the incoming airflow, and h_m is the average mountain height. In this case, $U = 20.0$ m s^{-1}, $Nw = 0.0098$ s^{-1}, $h_m = 4000$ m), which indicates that the impinging flow was only partially blocked by the terrain at low levels in the atmosphere (<2 km), consistent with the small area of stagnant flow in Figure 11A between the Ghaghra and Kali Gandaki valleys. Note the jet-like structure of the southerly flow along the Kali Gandaki (KG) and western Ghaghra (G) River valleys, which function as open conduits delivering atmospheric moisture to the northern flanks of the Himalayas. This behavior is consistent with results of covariance analysis of satellite imagery and topography suggesting that trans-Himalayan river valleys determine the multiscaling behavior of cloud fields in the Great Himalayas (Barros et al., 2004). Long-term indirect evidence of the along-valley channelization of atmospheric flows and associated precipitation is also patent in oxygen isotope (e.g., $\delta^{18}O_{mw}$) analysis of stream flow with respect to altitude along the Kali Gandaki River valley (Garzione et al., 2000).

Let us now focus on the simulated mesoscale cloud features during the northwestward movement of the monsoon depression. The simulation (Fig. 12) clearly depicts the distribution of maximum cloud liquid water in the vertical air column for the innermost domain (Δx = 1.86 km) at 12 UTC 12 June (left panel), and 00 UTC 13 June 1999 (right panel). Both windward and lee side of individual mountain peaks received a considerable amount of moisture when the monsoon depression reached the central Himalayas. Note how the organization of clouds fields exhibits a strong association with the spatial arrangement of topography. In particular, the highest liquid water content occurs along the major river valleys and along the windward flanks at middle latitudes (2–4 km) in the High Himalaya.

To gain further insight into the interactions between monsoon depression and orography, we now analyze the distribution of vertical velocity, cloud liquid water, and equivalent potential temperature in the innermost domain along the cross section traversing the Himalaya (section A–A*, Fig. 4B). Orographic forcing leads to the spatial organization of strong and deep updrafts in the foothills of the Himalayan range accompanied by the propagation of orographic gravity waves with updrafts concentrated on upwind slopes (S and SE facing slopes), while downdrafts dominate on top and on the lee side (N and NW facing slopes) of individual terrain peaks at 12 UTC 12 June (Fig. 13C). This topographically driven organization leads to the

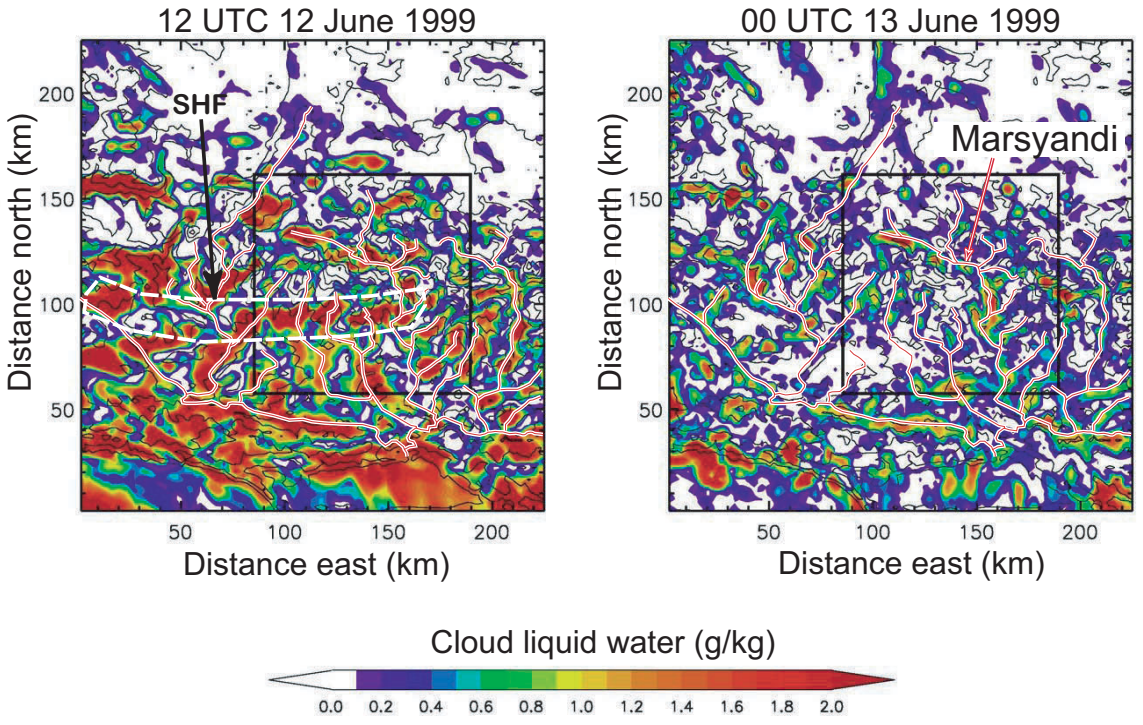

Figure 12. Simulated fields of maximum cloud water in the atmospheric column in the inner domain (domain 3, 1.86 km grid resolution) at 12 UTC 12 June 1999 (left panel), and 00 UTC 13 June 1999 (right panel). Dashed region delineates the southern Himalayan flank (SHF), where rain is intense.

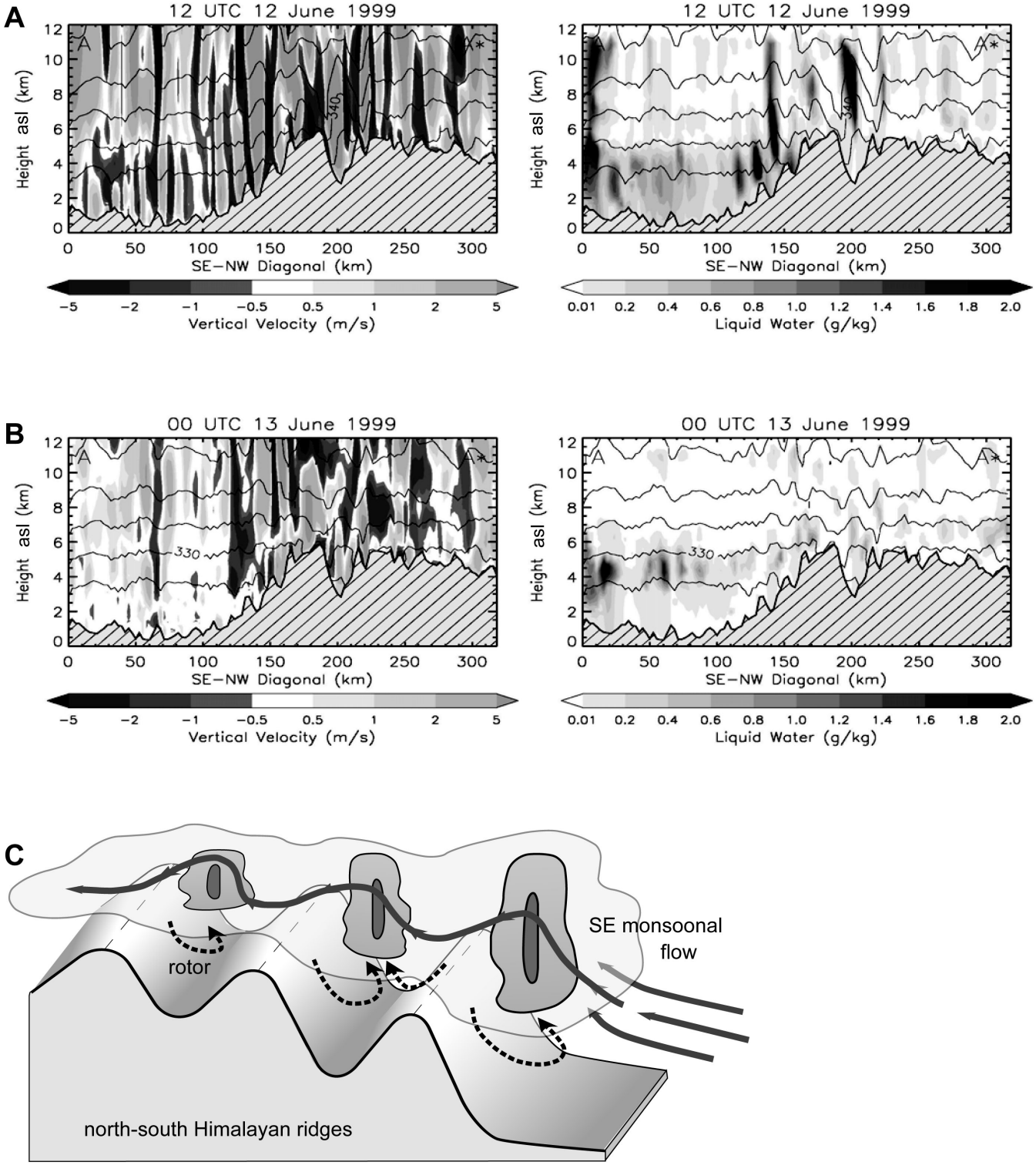

F

(g kg^{-1}): (A) 12 UTC 12 June 1999, and (B) 00 UTC 13 June 1999. The cross-section A–A* is depicted in Figure 4B. (C) Cartoon of the orographically induced gravity waves due to SE monsoon flows impinging obliquely on north-south–oriented ridges extending southward from the Himalayan crest. Forced ascending air focuses precipitation on the upwind (W to SW) slopes, with reduced rainfall on downwind slopes and some ridge crests.

formation of cells of high cloud water content, which extends northward into normally dry regions like the Tibetan Plateau at ~12 UTC 12 June (Fig. 13A). Twelve hours later, by 00 UTC 13 June (Fig. 13B), vertical motion weakened on the upwind slopes as the depression moved away toward the west, cutting off the influx of moisture and leading to significant changes in the distribution of cloud water at 00 UTC 13 June.

These results illustrate the role of monsoon depressions as a mechanism for transferring moisture (and latent heat energy) from the Bay of Bengal to the Himalayas and into Tibet. The effectiveness of this transport is controlled by the depression path, and by the number (frequency) of depressions that originate from the Bay of Bengal during the summer monsoon. Over long time scales, and even for different global climate regimes (Bradley, 1991; Kutzbach et al., 1993; Clemens et al., 1991; among others), we propose that the path and number of monsoon depressions that reach the mountain range and penetrate beyond the upwind crest can be used as predictive measures of monsoon intensity. Such events determine precipitation accumulation in existing glaciers (Harper and Humphrey, 2003), the formation of new glaciers, as well as altitudinal-dependent erosion patterns and mechanisms (landslides, river incision rates), thereby potentially influencing landscape evolution (Gabet et al., 2004).

2001 Monsoon Onset

The simulation of the 2001 monsoon onset began at 00 UTC 12 June and ran for 48 h. Model results of wind fields 1.5 km above the ground surface at 00 UTC 13 June and 00 UTC 14 June are shown in Figures 14A and 14B, respectively. The simulation results indicate a cyclonic flow around the northeast coast of India on 00 UTC 13 June (Fig. 14A), a result consistent with the ECMWF analysis (Fig. 8A). By 00 UTC 14 June 2001 (Fig. 14B), the cyclonic circulation remained stationary (Fig. 8B). Overall, the model is able to predict well the location of the monsoon depression over northeast India. The left and right panels in Figure 15 show the maximum cloud water at 00 UTC 13 and 00 UTC 14 June 2001, respectively. Although cells of cloud liquid water formed in the vicinity of individual mountain peaks, large areas in the central Himalayas were not affected by the monsoon depression directly and show clear skies. The southwest to northeast cross sections of simulated vertical

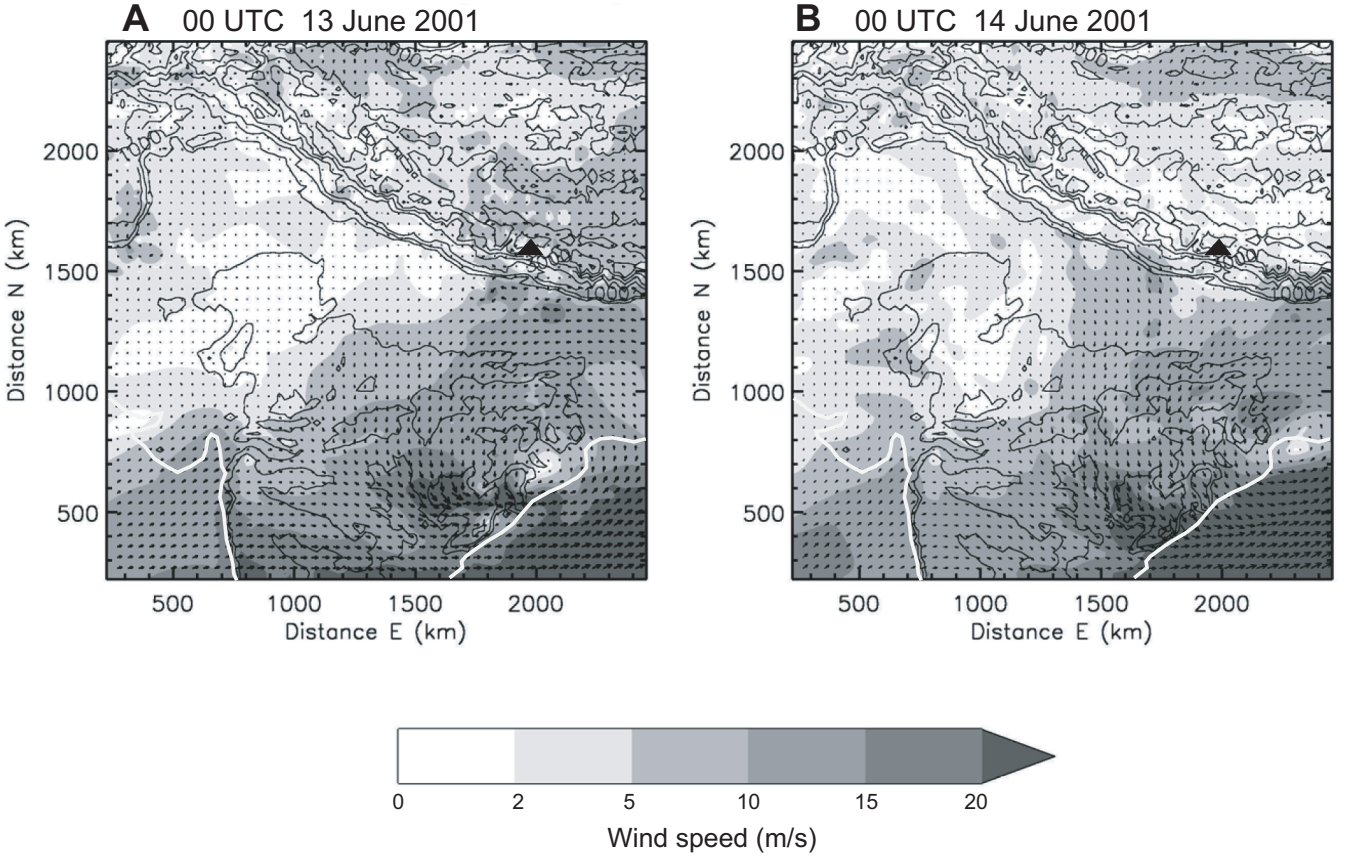

Figure 14. Simulated wind streamlines and wind speed (shaded) 1.5 km above the ground surface for the outer domain (domain 1, 22.22 km grid resolution) at (A) 00 UTC 13 June 2001, and (B) 00 UTC 14 June 2001. Contours show orography in increments of 1000 m. Black triangles mark the approximate location of the network.

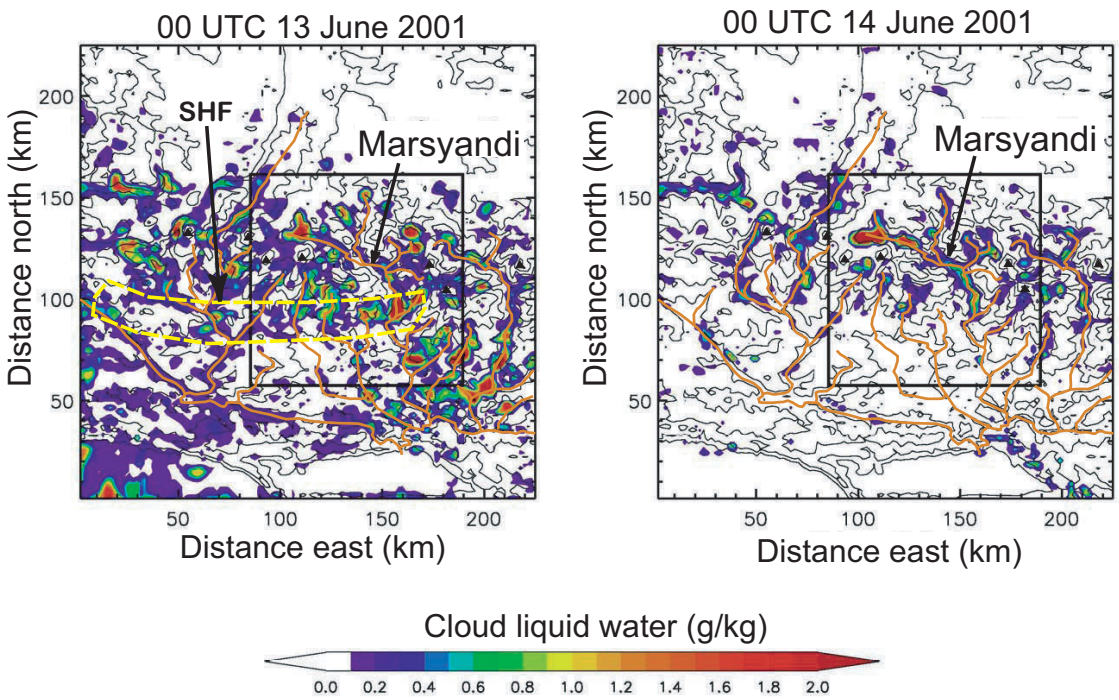

Figure 15. Simulated fields of maximum cloud water in the atmospheric column in the inner domain (domain 3, 1.86 km grid resolution) at 00 UTC 13 June 2001 (left panel), and 00 UTC 14 June 2001 (right panel). Note the significantly reduced precipitation along the southern Himalayan flank (SHF) in comparison to the monsoon onset of June 1999 (Fig. 12).

motion and cloud liquid water (Fig. 16) show that the moisture flux over the complex terrain is much reduced as compared to that in 1999. As a consequence, precipitation is very light over the Himalayan range in general, and on the upwind slopes in particular. The one-to-one correspondence between the magnitude and spatial distribution of the updrafts and the spatial arrangement of successive valleys and ridges shows the importance of orographic gravity waves in organizing local circulations despite weak synoptic forcing. As the monsoon depression moved westward during 14 June 2001, the cloud liquid water reduced dramatically everywhere (Fig. 15, right panel). During that time, a band-like feature of high cloud water content (~2.0 g kg^{-1}) is simulated over the upper Marsyandi Valley, as a result of up-valley easterly flow (Fig. 14B). As shown in Figure 16B, strong vertical motion is simulated at high elevations around 00 UTC 14 June 2001, while it is very weak along the front range. Consequently, cloud water content is very low everywhere due to the lack of sustained moisture influx into the region.

In summary, the numerical simulations predict that orographically organized convection (Fig. 13C) is a persistent feature of weather in the Great Himalayas, as previously inferred from the analysis of satellite imagery over a wide range of scales (Barros et al., 2004). Nevertheless, significant summertime precipitation only occurs when strong and sustained moisture transport into the region is established by environmental conditions associated with strong monsoon depressions (and onsets in particular) on a collision path with the orographic barrier. Moreover, deep penetration of monsoon moisture into the rain shadow north of the high Himalayan summits is predicted to occur only when the monsoon depression impinges directly on the range front, and moisture convergence is channelized along the major river valleys. Therefore, the summertime mass input to the glaciers located at high elevations and sprawling into the northern flanks of the Himalayas and southern Tibet is conditioned on the occurrence of such discrete events.

2000 Winter Storm

The simulation started at 00 UTC 11 February and ran for 36 h. The simulated horizontal wind fields 1.5 km above the ground surface for a portion of the outer model domain at 06 UTC 11 February 2000 (Fig. 17A) and 00 UTC 12 February 2000 (Fig. 17B) show the evolution of a southwesterly low-level jet impinging on the central Himalayas at 10–15 ms^{-1}. This low-level jet is associated with the cyclonic flow around the shallow depression, and turns slightly westward as it approaches the orographic barrier. Although the westward turning of low-level flow was not as significant as in the ECMWF analysis (Fig. 10), the model successfully captures the timing of the storm in central Nepal from 06 UTC to 12 UTC 12 February 2000.

The spatial distribution of maximum cloud water in the innermost model domain is shown in Figure 18. By 06 UTC 11 February (Fig. 18, left panel), scattered clouds are present over

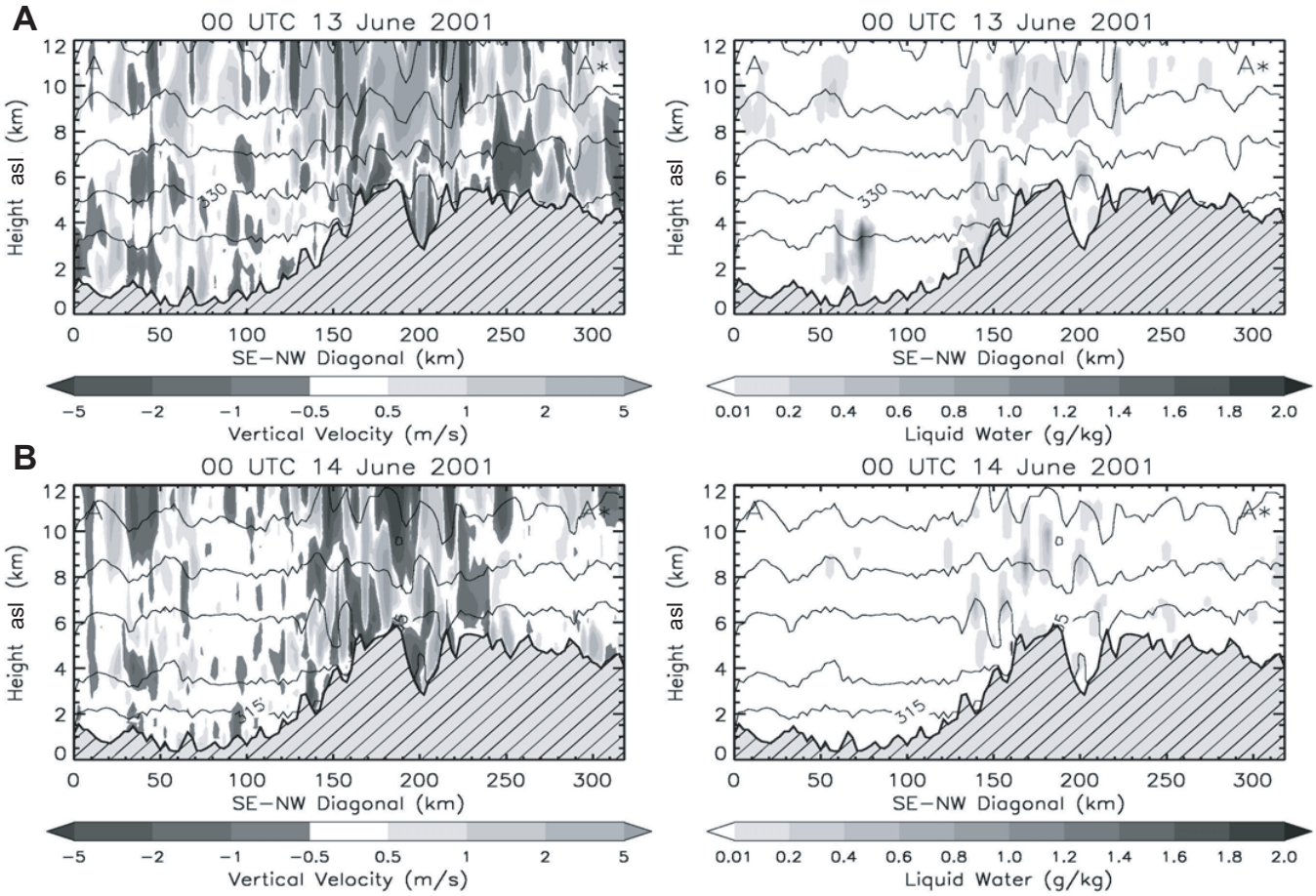

the network area, especially over the Annapurnas, with a long linear cloud feature on the windward side, a feature consistent with forced orographic lifting along the Lesser Himalayas in the absence of environmental instability (i.e., no embedded convection). Subsequently, clouds developed around isolated mountain peaks (Fig. 18, right panel) as the trough moved eastward. Note that, in contrast to the monsoon onset events (Figs. 12 and 15), cloud formation along the Marsyandi Valley during the passage of the winter trough is negligible (Fig. 18). Instead, moisture is focused on the surrounding ridges as a result of sustained strong southwesterly flow (Fig. 17) that leads to the development of strong downdrafts in the valley by 00 UTC 12 February.

Cross sections of simulated vertical velocity and cloud water content along the cross-section A–A* (Fig. 4B) are presented in Figure 19. Again, as in the case of monsoon depressions, these results suggest that vertical motion is strongly tied to orographic features, consistent with the generation of orographic gravity waves from the interaction between the impinging air mass and the Himalayan range on 06 UTC 11 February (Fig. 19A) and 00 UTC 12 February 2000 (Fig. 19B), respectively. Note the persistent cloud features in the Lesser Himalayas (Fig. 19), where linear zones of concentrated moisture are predicted (Fig. 18). The vertical cross section of cloud liquid water distribution reveals shallow clouds on 11 and 12 February 2000 (Figs. 19A and 19B), similar to cloudiness fields derived from METEOSAT-IR imagery (see Lang and Barros, 2004, for details). Consequently, precipitation amounts produced by this cold season storm are substantially lower than those attained during the 1999 onset events, though higher than during the 2001 onset. The average number of wintertime storms is on the order of a handful per year, and their cumulative contribution to annual precipitation is significant, especially at high elevations (as much as 100 cm for elevations above 3500 m in the Marsyandi network; Fig. 1B).

OVERVIEW AND DISCUSSION

We have characterized the complexity and space-time intermittency of precipitation in the central Himalayas via a combina-

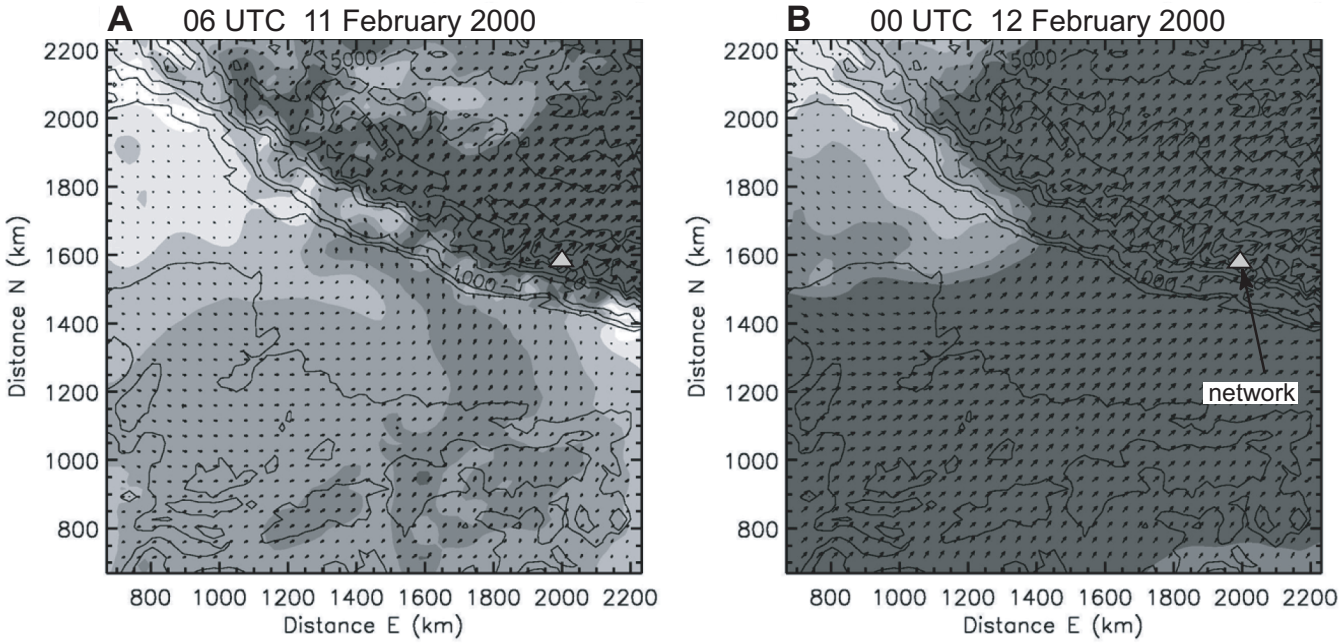

Figure 17. Simulated wind streamlines (vectors) and wind speed (shaded) 1.5 km above the ground surface for the outer domain (domain 1, 22.22 km grid resolution) at (A) 06 UTC 11 February 2000, and (B) 00 UTC 12 February 2000. Contours show orography in increments of 1000 m. Gray triangles mark the approximate location of the network.

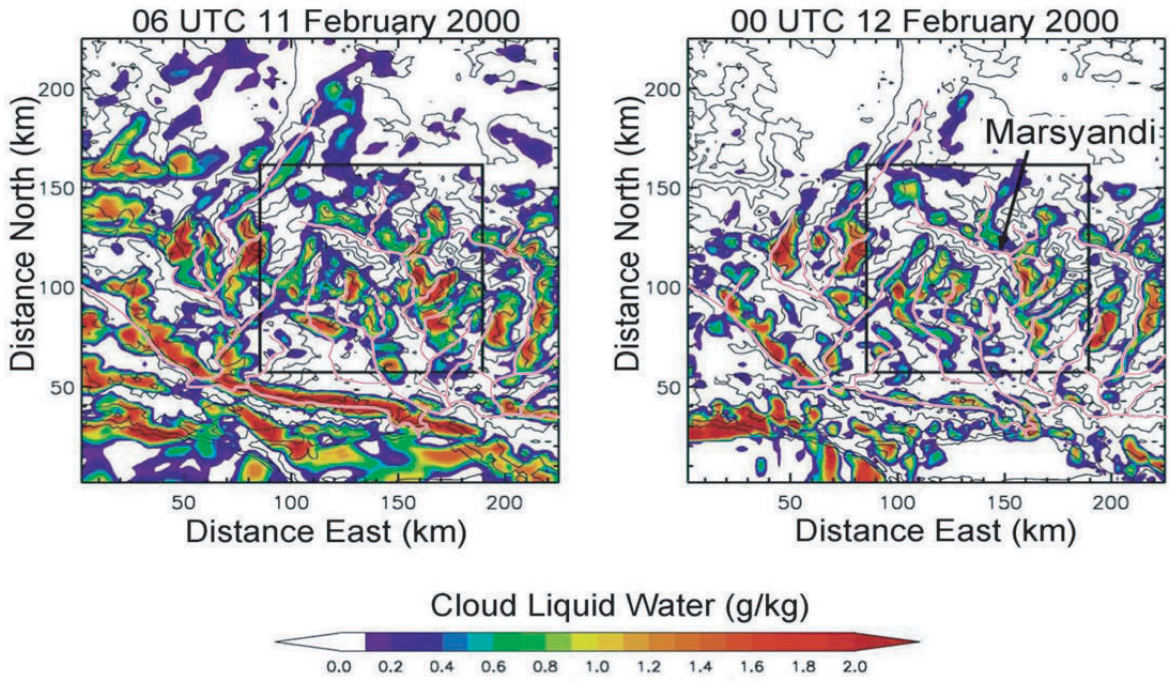

Figure 18. Simulated fields of maximum cloud water in the atmospheric column in the inner domain (domain 3, 1.86 km grid resolution) at 06 UTC 11 February (left panel), and 00 UTC 12 February 2000 (right panel). Note that, in comparison to monsoon simulations (Figs. 12 and 15), much precipitation is focused on ridges, rather than along river valleys

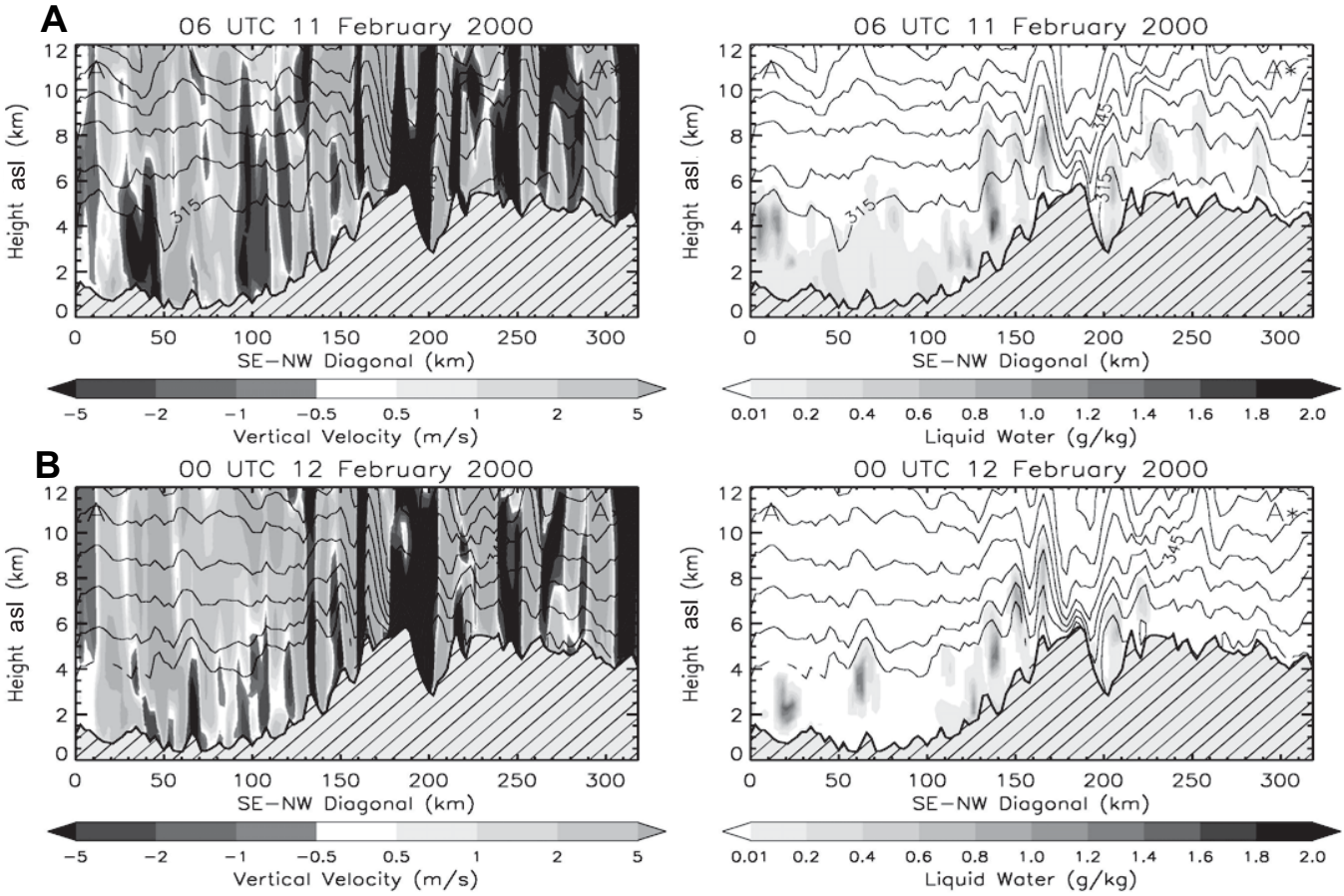

Figure 19. Simulated *x-z* cross section of vertical velocity (m s^{-1}), potential temperature (contour interval 10 K), and cloud liquid water content (g kg^{-1}): (A) 06 UTC 11 February, and (B) 00 UTC 12 February 2000. The cross-section A–A* is depicted in Figure 4B.

tion of ground observations, satellite imagery, and model simulations of dominant weather systems for current climate conditions. The role of orographic land-atmosphere interactions in the spatial organization of precipitation systems is exemplified by three fundamental modes of spatial variability: a synoptic-scale mode linked to global climate controls; a synoptic-scale mode linked to regional climate controls related to monsoon intensity and landform; and finally, a mesoscale mode linked to local orography (Barros et al., 2004). In this work, we show how independent model simulations of representative weather events (monsoon depression and wintertime storms) appear to effectively capture the synoptic and mesoscale modes of variability.

Depending on wind direction, flow over the terrain creates a unique pattern of gravity waves, with vertical motion forming band-like structures oriented roughly parallel to the dominant topographic ridges, which force the waves. Environmental conditions favor the formation of vertically deep waves, with phase lines that tilt into the wind, leading to the simulated phase difference between topography and vertical motion consistent with the theory of Smith (1979). These waves influence cloud heights, as lower cloud tops often are associated with ridges, and higher cloud tops over the intervening slopes. Cloud liquid water content (and by inference rainfall) is maximized where updrafts and the potential temperature gradient are stronger. The simulated spatial patterns of rainfall are consistent with observations from both monsoon onsets, which suggests that that orographic lifting is the key rainfall process (Lang and Barros, 2002). Depending on the synoptic conditions, the gravity wave cells of vertical motion would be expected to modulate the intensity of any incoming convective activity, as well as to prompt the localized release of low-level convective instability in the regions of forced ascent (Barros and Lang, 2003a). This is consistent with the results from Reinking et al. (2000), who showed that orographically produced gravity waves can have important effects on rainfall.

Although a much longer numerical integration is required to fully elucidate the effects of radiative processes and terrain-atmosphere interactions over longer time scales, these model simulations of principal weather systems imply a strong association between rainfall and spatial wind patterns modulated by orography. This association is supported by the analysis of satellite imagery of clouds. Thus, we should expect relative distributions of rainfall on the southern slopes to remain constant from

year to year (although absolute amounts will be subject to the interannual variability of the Asian monsoon itself). This inference is further supported by the observations of Lang and Barros (2002), Barros and Lang (2003a), and Barros et al. (2004), who found that relative rainfall distributions remained stable in 1999, 2000, and 2001 in the Marsyandi network. On the northern slopes and in the hydrometeorological rain shadow (Fig. 1B), the temporal scales at which spatial patterns of cumulative precipitation remain stable are at least on the order of decades, consistent with multidecadal variability of the monsoon. Overall, analysis and integration of ground observations, satellite imagery, and model simulations of dominant weather systems for current climate conditions emphasize the need to describe and interpret climate records accounting for chaotic and stochastic variability over a wide range of temporal and spatial scales (frequency, intensity, path distributions of monsoon depressions, and spatial distribution of associated rainfall).

At geologic time scales, a spatially fixed rainfall distribution should have significant effects on erosion and geomorphology, suggesting an interesting long-term feedback between the terrain and atmosphere. For example, persistently greater intensity and magnitude of rainfall on southeasterly flanks of ridges could lead to lower channel slopes, interfluve heights (Whipple et al., 1999), and hillslope angles (Gabet et al., 2004). Furthermore, indirect evidence of spatial consistency between active deformation and heavy rainfall patterns in the Himalayas suggests that this feedback may impact the spatial organization of tectonic activity (Hodges et al., 2004).

Despite recent progress in characterizing the spatial variability of precipitation in major mountain ranges like the Himalayas, the detailed structure of that variability and the fundamental spatial and temporal modes of climate change have remained poorly defined. Similarly, the extent to which orography may be a product of climate-erosion interactions is unknown (Burbank et al., 2003; Reiners et al., 2003; Wobus et al., 2003). Many landscape models either assume a uniform distribution of precipitation (Willett, 1999; Ellis et al., 1999), gradients in precipitation as a function of horizontal distance (Beaumont et al., 2000; Jamieson et al., 2002), or step-wise changes between domains of uniform precipitation (Willett, 1999; Ellis et al., 1999). Some conceptual models assume a homogeneous variation of annual precipitation with elevation, consistent with uniform orographic enhancement of rainfall across a mountain range (Roe et al., 2003). Both our observations and modeling in the Himalaya show strong spatial variability in precipitation at the scale of individual ridges and valleys that serve as obstacles to incoming storms. Our work suggests that annual precipitation averages might be considered appropriate approximations of climate gradients only for mountain ranges oriented perpendicular to the major storm tracks, because moisture is advected directly toward the range crest (i.e., north-south orientation such as occurs for the Rocky Mountains with respect to the prevailing westerlies). Furthermore, the representation of orographic enhancement of rainfall in terms of a linear dependence with elevation neglects the contribution of orography to organize and enhance convective activity, which is responsible for the diurnal cycle of rainfall in mountainous regions, and for spatially persistent heavy precipitation in particular (e.g., the so-called "cloud bursts" in the Himalayas; Barros et al., 2004). Montgomery and Brandon (2002) suggested that frequency in landsliding plays a major role in controlling landscape-scale erosion in tectonically active mountain ranges. Because landsliding activity can be often linked to heavy precipitation (Gabet et al., 2005), the frequency and spatial pattern of orographic convective precipitation must not be ignored.

Simulations using global climate models, with and without the Himalayas and Tibetan Plateau, indicate that the mountains do not have an influence on whether the monsoon takes place (e.g., Zhisheng et al., 2001; Kitoh, 2001; Abe et al., 2003). However, they do show that the presence of the mountains contributes to lengthening the duration of the monsoon; for simulations using different average terrain elevations, more elevated mountain ranges are correlated with earlier monsoon onsets and more intense monsoons (Hahn and Manabe, 1975; Kutzbach et al., 1993; Zhisheng et al., 2001; and many others). We propose that, whereas global climate controls (solar insolation, land-mass distribution, ice-sheet distribution) effectively determine glacial and interglacial oscillations, the characteristics of interannual variability of precipitation for modern climate conditions are reflective of the potential range of variability of climate controls under climate regimes associated with strong monsoon activity (interglacial periods). Under weak monsoon regimes, the effective height of the mountains as an elevated heat source is depressed and constrained to lower elevations in the troposphere. More specifically, during glacial periods, colder sea-surface temperatures and a decrease in land-ocean temperature contrast should lead to a decrease in atmospheric moisture transport during the monsoon, decrease in the moisture-holding capacity of the atmosphere, decrease of the overall accumulation of precipitation, increase in the relative fraction of solid precipitation at lower elevations, and possibly reduced interannual variability in the tropics. This would imply a glacial-age southward shift of the hydrometeorological crest and shortening of the penetration distance of incoming moisture into the hydrometeorological rain shadow. This scenario is consistent with the greater snowline lowering observed for glaciers south of the range crest (Burbank et al., 2003), although the sensitivity of the high-elevation glaciers to seasonal and subseasonal variability of precipitation might remain similar to that for modern climate.

Nevertheless, independently of the monsoon regime, local precipitation amounts and spatial gradients of precipitation should be anchored by their contemporaneous topography. The outstanding questions of how this two-way feedback between mountains and the atmosphere impacts erosion processes, and how erosion and tectonics interact over millions of years to produce modern topography (and hydrometeorology), require an end-to-end integrated study from the dominant spatial scales of precipitation to the orogen scale.

ACKNOWLEDGMENTS

This research was funded over the last five years by the National Aeronautics and Space Administration Tropical Rainfall Measurement Mission (NASA-TRMM) (NAG5-7781) and National Aeronautics and Space Administration Precipitation Measurement Missions (NASA-PMM) (NNG04GP02G), and by the National Science Foundation Continental Dynamics program (EAR-9909647 and EAR-9909498). This work benefited from discussions with K. Hodges, M. Strecker, T.N. Krishnamurti, J. Matsumoto, B. Pratt-Sitaula, N. Humphrey, E. Gabet, and B. Bookhagen.

REFERENCES CITED

Abe, M., Kitoh, A., and Yasunari, T., 2003, An evolution of the Asian summer monsoon associated with mountain uplift simulation with the MRI atmosphere-ocean coupled GCM: Journal of the Meteorological Society of Japan, v. 81, p. 909–933, doi: 10.2151/jmsj.81.909.

Barros, A.P., and Lang, T.J., 2003a, Monitoring the monsoon in the Himalayas: Observations in central Nepal, June 2001: Monthly Weather Review, v. 131, p. 1408–1427, doi: 10.1175/1520-0493(2003)131<1408:MTMITH>2.0.CO;2.

Barros, A.P., and Lang, T., 2003b, Exploring spatial modes of variability of terrain-atmosphere interactions in the Himalayas during monsoon onset: Environmental Sciences and Engineering Program, Division of Engineering and Applied Sciences, Harvard University, Hydrosciences Report Series, no. 03-001, 51 p.

Barros, A.P., Joshi, M., Putkonen, J., and Burbank, D.W., 2000, A study of the 1999 monsoon rainfall in a mountainous region in central Nepal using TRMM products and rain gauge observations: Geophysical Research Letters, v. 27, p. 3683–3686, doi: 10.1029/2000GL011827.

Barros, A.P., Kim, G., Williams, E., and Nesbitt, S.W., 2004, Probing orographic controls in the Himalayas during the monsoon using satellite imagery: Natural Hazards and Earth Systems Science, v. 4, p. 1–23.

Beaumont, C., Munoz, J.A., Hamilton, J., and Fullsac, P., 2000, Factors controlling the Alpine evolution of the central Pyrenees inferred from a comparison of observations and geodynamical models: Journal of Geophysical Research, v. 105, p. 8121–8145, doi: 10.1029/1999JB900390.

Bradley, R.S., 1991, Paleoclimatology: International Geophysics Series, Prentice-Hall, v. 64, 611 p.

Burbank, D.W., Blythe, A.E., Putkonen, J., Pratt, B., Gabet, E., Oskin, M., Barros, A., and Ojha, T.P., 2003, Decoupling of erosion and precipitation in the Himalaya: Nature, v. 426, p. 652–655, doi: 10.1038/nature02187.

Clark, T.L., 1979, Numerical simulations with a three-dimensional cloud model: Lateral boundary condition experiments and multi-cellular severe storm simulations: Journal of Atmospheric Sciences, v. 36, p. 2191–2215, doi: 10.1175/1520-0469(1979)036<2191:NSWATD>2.0.CO;2.

Clark, T.L., and Hall, W.D., 1991, Multi-domain simulations of the time dependent Navier Stokes equations: Benchmark error analyses of some nesting procedures: Journal Computational Physics, v. 92, p. 456–481.

Clark, T.L., and Hall, W.D., 1996, The design of smooth, conservative vertical grids for interactive grid nesting with stretching: Journal of Applied Meteorology, v. 35, p. 1040–1046, doi: 10.1175/1520-0450(1996)035<1040:TDOSCV>2.0.CO;2.

Clark, T.L., Hall, W.D., and Coen, J.L., 1996, Source code documentation for the Clark-Hall cloud-scale model code version G3CH01: Boulder, Colorado, National Center for Atmospheric Research Technical Note NCAR/TN-426+STR.

Clemens, S., Prell, W., Murray, D., Shimmield, G., and Weedon, G., 1991, Forcing mechanisms of the Indian Ocean monsoon: Nature, v. 353, p. 720–725, doi: 10.1038/353720a0.

Das, P.K., 1987, Short and long-range monsoon prediction in India, *in* Fein, J.S., and Stephens, P.L., eds., Monsoons: New York, John Wiley & Sons, p. 549–578.

Duan, K., and Yao, T., 2003, Monsoon variability in the Himalayas under the condition of global warming: Journal of the Meteorological Society of Japan, v. 81, no. 2, p. 251–257, doi: 10.2151/jmsj.81.251.

Ellis, M.A., Densmore, A.L., and Anderson, R.S., 1999, Development of mountainous topography in the Basin Ranges, USA: Basin Research, v. 11, p. 21–41, doi: 10.1046/j.1365-2117.1999.00087.x.

Gabet, E.J., Pratt-Sitaula, B.A., and Burbank, D.W., 2004, Climatic controls on hillslope angle and relief in the Himalayas: Geology, v. 32, p. 629–632, doi: 10.1130/G20641.1

Gabet, E.J., Burbank, D.W., Putkonen, J., Pratt-Sitaula, B.A., and Ojha, T., 2005, Rainfall thresholdings for landsliding in the Himalayas of Nepal: Geomorphology, v. 63, p. 131–143.

Garzione, C.N., Quade, J., DeCelles, P.G., and English, N.B., 2000, Predicting paleoelevation of Tibet and the Himalaya from $\delta^{18}O$ vs. altitude gradients in meteoric water across the Nepal Himalaya: Earth and Planetary Science Letters, v. 183, p. 215–229, doi: 10.1016/S0012-821X(00)00252-1.

Hahn, D.G., and Manabe, S., 1975, The role of mountains in the South Asian Monsoon Circulation: Journal of the Atmospheric Sciences, v. 32, no. 8, p. 1515–1541.

Harper, J., and Humphrey, N.F., 2003, High altitude Himalayan climate inferred from glacial ice flux: Geophysical Research Letters, v. 30, doi: 10.1029/2003GL017329.

Hodges, K.V., Wobus, C., Ruhl, K., Schilgden, T., and Whipple, K., 2004, Quaternary deformation, river steepening, and heavy precipitation at the front of the Higher Himalayan ranges: Earth and Planetary Science Letters, v. 220, p. 379–389, doi: 10.1016/S0012-821X(04)00063-9.

Jamieson, R.A.B., Nguyen, M.H., and Lee, B., 2002, Interaction of metamorphism, deformation and exhumation in large convergent orogens: Journal of Metamorphic Geology, v. 20, p. 9–24, doi: 10.1046/j.0263-4929.2001.00357.x.

Kessler, E., 1969, On the distribution and continuity of water substance in atmospheric circulations: American Meteorological Society, Meteorological Monographs, no. 32, 84 p.

Kitoh, A., 2001, Effect of orography on land and ocean surface temperature: Present and future of modeling global environmental change, *in* Matsuno, T., and Kida, H., eds., Toward integrated modeling: TERRAPUB, p. 427–431.

Krishnamurti, T.N., Ardanuy, P., Ramanathan, Y., and Pash, R., 1981, On the onset vortex of the summer monsoon: Monthly Weather Review v. 109, p. 344–363, doi: 10.1175/1520-0493(1981)109<0344:OTOVOT>2.0.CO;2.

Kutzbach, J.E., Prell, W.L., and Ruddiman, W.F., 1993, Sensitivity of Eurasian climate to surface uplift of the Tibetan Plateau: Journal of Geology, v. 101, p. 177–190.

Lang, J.T., and Barros, A.P., 2002, An investigation of the onsets of the 1999 and 2000 monsoons in central Nepal: Monthly Weather Review, v. 130, p. 1299–1316.

Lang, J.T., and Barros, A.P., 2004, Winter storms in the central Himalayas: Journal of the Meteorological Society of Japan, v. 82, p. 829–844, doi: 10.2151/jmsj.2004.829.

Magagi, R., and Barros, A.P., 2004, Estimation of Latent heating of rainfall during the onset of the Indian monsoon using TRMM-PR and radiosonde data: Journal of Applied Meteorology, v. 43, no. 2, p. 328–349, doi: 10.1175/1520-0450(2004)043<0328:EOLHOR>2.0.CO;2.

Molnar, P., England, P., and Martinod, J., 1993, Mantle dynamics, uplift of the Tibetan Plateau, and the Indian monsoon: Reviews in Geophysics, v. 31, p. 357–396, doi: 10.1029/93RG02030.

Montgomery, D.R., and Brandon, M.T., 2002, Topographic controls on erosion rates in tectonically active mountain ranges: Earth and Planetary Science Letters, v. 201, p. 481–489, doi: 10.1016/S0012-821X(02)00725-2.

Pinter, N., and Brandon, M.T., 1997, How erosion builds mountains: Scientific American, April 1997, p. 74–79.

Reiners, P.W., Ehlers, T.A., Mitchell, S.G., and Montgomery, D.R., 2003, Coupled spatial variations in precipitation and long-term erosion rates across the Washington Cascades: Nature, v. 426, p. 645–647, doi: 10.1038/nature02111.

Reinking, R.F., Snider, J.B., and Coen, J.L., 2000, Influences of storm-embedded orographic gravity waves on cloud liquid water and precipitation: Journal of Applied Meteorology, v. 39, p. 733–759, doi: 10.1175/1520-0450(2000)039<0733:IOSEOG>2.0.CO;2.

Roe, G.H., Montgomery, D.R., and Hallet, B., 2003, Orographic precipitation and the relief of mountain ranges: Journal of Geophysical Research, v. 108, paper no. 2315, doi: 10.1029/2001JB001521.

Sasamori, T., 1972, A linear harmonic analysis of atmospheric motion with radiative dissipation: Journal of the Meteorological Society of Japan, v. 50, p. 505–517.

Smith, R.B., 1979, The influence of mountains on the atmosphere: Advances in Geophysics, v. 21, p. 87–230.

Stephens, G., 1984, Short-wave parameterization revised to improve cloud absorption: Journal of Atmospheric Sciences, v. 41, p. 687–690, doi: 10.1175/1520-0469(1984)041<0687:ASPRTI>2.0.CO;2.

Tang, M., and Reiter, E.R., 1984, Plateau monsoons of the Northern Hemisphere: A comparison between North America and Tibet: Monthly Weather Review, v. 112, p. 617–637.

Thompson, L.G., Yao, T., Mosley-Thompson, E., Davis, M.E., Henderson, K.A., and Lin, P.-N., 2000, A high-resolution millennial record of the south Asian monsoon from Himalayan ice cores: Science, v. 289, p. 1916–1919.

Whipple, K., Kirby, E., and Brocklehurst, S., 1999, Geomorphic limits to climate-induced increases in topographic relief: Nature, v. 401, p. 39–43, doi: 10.1038/43375.

Willett, S.D., 1999, Orogeny and orography—The effects of erosion on the structure of mountain belts: Journal of Geophysical Research, v. 104, p. 28,957–28,981, doi: 10.1029/1999JB900248.

Wobus, C.W., Hodges, K.V., and Whipple, K.X., 2003, Has focused denudation sustained active thrusting at the Himalayan topographic front?: Geology, v. 31, p. 861–864, doi: 10.1130/G19730.1.

Zhao, H., and Moore, G.W.K., 2002, On the relationship between Dasuopu snow accumulation and the Asian summer monsoon: Geophysical Research Letters, v. 29, 2222, doi: 10.1029/2002GL015757.

Zhisheng, A., Kutzbach, J.E., Prell, W.L., and Porters, S.C., 2001, Evolution of Asian monsoons and phased uplift of the Himalaya-Tibetan Plateau since late Miocene times: Nature, v. 411, p. 62–66, doi: 10.1038/35075035.

Manuscript Accepted by the Society 23 June 2005

Printed in the USA